AD

USAAVLABS TECHNICAL REPORT 64-68J

HEAVY-LIFT TIP TURBOJET ROTOR SYSTEM
VOLUME X
STABILITY AND CONTROL

October 1965

U. S. ARMY AVIATION MATERIEL LABORATORIES
FORT EUSTIS, VIRGINIA

CONTRACT DA 44-177-AMC-25(T)
HILLER AIRCRAFT COMPANY, INC.

Task 1M121401D14412
Contract DA 44-177-AMC-25(T)
USAAVLABS Technical Report 64-68J
October 1965

HEAVY-LIFT TIP TURBOJET ROTOR SYSTEM

VOLUME X

STABILITY AND CONTROL

Hiller Engineering Report No. 64-50

Prepared by

Hiller Aircraft Company, Inc.
Subsidiary of Fairchild Hiller Corporation
Palo Alto, California

For

U. S. ARMY AVIATION MATERIEL LABORATORIES
FORT EUSTIS, VIRGINIA

(U. S. Army Transportation Research Command when report prepared)

CONTENTS

ILLUSTRATIONS

ILLUSTRATIONS (CONTINUED)

TABLES

SYMBOLS

a	Rotor blade section lift curve slope
a_t	Horizontal stabilizer lift curve slope
A_π	Fuselage equivalent flat plate area
c	Blade chord
C_{D_o}	Rotor blade section profile drag coefficient
$C_{D_{TT}}$	Tip-mounted engine nacelle drag coefficient (based on inlet area)
c.g.	Center of gravity
C_ℓ	Rolling moment coefficient $= \dfrac{\ell}{\frac{1}{2}\rho V^2 \pi R^2 (2R)}$
C_L	Lift coefficient $= \dfrac{L}{\frac{1}{2}\rho V^2 S}$
$\left(\dfrac{\partial C_L}{\partial \alpha}\right)_{TT}$	Tip-mounted engine nacelle lift curve slope (based on inlet area)
C_{M_f}	Fuselage pitching moment coefficient $= \dfrac{M_f}{\frac{1}{2}\rho V^2 \pi R^2 (R)}$
C_N	Yawing moment coefficient $= \dfrac{N}{\frac{1}{2}\rho V^2 \pi R^2 (2R)}$
C_T	Thrust coefficient $= \dfrac{T}{\rho(\pi R^2)\Omega^2 R^2}$
C_X	Horizontal force coefficient $= \dfrac{X}{\rho(\pi R^2)\Omega^2 R^2}$
$c_{\frac{1}{2}x}$	Cycles to half amplitude
c_{2x}	Cycles to double amplitude
C_Y	Side force coefficient $= \dfrac{Y}{\frac{1}{2}\rho V^2 \pi R^2}$
d	Distance from blade c.g. to flapping hinge

e	Flapping hinge offset
"e"	Equivalent flapping hinge offset (relates main rotor spring restraint to an equivalent offset hinge)
e_f	Distance of c.g. forward of main rotor hub
g	Acceleration due to gravity
h	Distance of main rotor hub above c.g.
i_t	Incidence angle of horizontal stabilizer with respect to fuselage centerline(positive leading edge up)
I_b	Blade moment of inertia
$I_{\bar{x}\bar{x}}$	Moment of inertia about the $\bar{x}$-$\bar{x}$ axis
$I_{\bar{y}\bar{y}}$	Moment of inertia about the $\bar{y}$-$\bar{y}$ axis
$I_{\bar{z}\bar{z}}$	Moment of inertia about the $\bar{z}$-$\bar{z}$ axis
$I_{\bar{x}\bar{z}}$	Product of inertia $\int \bar{x}\bar{z}\, dm$
k_β	Spring restraint constant per blade, pound-feet/radian
ℓ_t	Distance of horizontal stabilizer quarter chord aft of c.g.
ℓ	Rolling moment
L	Lift force
m	Helicopter mass
m_b	Mass of one blade
M_{cg}	Pitching moment about c.g., positive nose up
M_f	Pitching moment about c.g. due to fuselage
M_{mr}	Pitching moment about c.g. due to main rotor
M_{s_y}	Pitching moment about c.g. due to spring restraint
M_t	Pitching moment about c.g. due to horizontal stabilizer
M_y	Pitching moment about c.g. due to offset hinge
b	Number of blades

N	Yawing moment
n_x	Longitudinal acceleration
n_z	Normal acceleration
$\hat{q}_o$	$= \frac{1}{2}\rho(\mu\Omega R)^2$
$\hat{q}_f$	$= \frac{1}{2}\rho(\mu\Omega R)^2 + \frac{1}{2}\rho V_i^2$
$\hat{q}_t$	$= \frac{1}{2}\rho(\mu\Omega R)^2 + \frac{1}{2}\rho(V_i)_t^2$
R	Main rotor radius
s	Laplace transform operator
S	Reference area
S_t	Horizontal stabilizer area
S_{TT}	Tip-mounted engine inlet area
$t_{\frac{1}{2}x}$	Time to half amplitude
t_{2x}	Time to double amplitude
T	Thrust
u	Perturbation of U
U	Linear velocity along the $\bar{x}$-$\bar{x}$ axis
V_T	Rotor tip speed
v	Perturbation of V
V	Linear velocity along the $\bar{y}$-$\bar{y}$ axis
$\bar{V}'$	Velocity vector of helicopter mass center
V_i	Induced velocity at main rotor
$(V_i)_t$	Induced velocity at horizontal stabilizer due to main rotor
w	Perturbation of W
W	Linear velocity along $\bar{z}$-$\bar{z}$ axis
W_G	Helicopter gross weight

X	Horizontal force (positive aft)
X_f	Horizontal force on fuselage
X_{mr}	Horizontal force on main rotor
X_{TT}	Resultant force due to airloads on tip mounted engine nacelles
x-x	Horizontal reference axis (fixed in space)
$\bar{x}$-$\bar{x}$	Longitudinal body* axis
$\bar{x}$	Distance parallel to $\bar{x}$-$\bar{x}$ axis from helicopter c.g. to component of interest, positive aft of c.g.
Y	Side force, parallel to $\bar{y}$-$\bar{y}$ axis, positive to the right
$\bar{y}$-$\bar{y}$	Lateral body* axis
Z	Vertical force, positive down
z-z	Vertical reference axis (fixed in space)
$\bar{z}$-$\bar{z}$	Vertical body* axis
$\bar{z}$	Distance parallel to $\bar{z}$-$\bar{z}$ axis from helicopter c.g. to component of interest, positive above c.g.
α_1	Forward tilt of rotor shaft with respect to z-z axis, positive tilt forward
α_f	Angle of attack of fuselage with respect to relative wind
β_ψ	Blade flapping angle at azimuth ψ relative to horizontal reference plane $= \beta_o + \beta_1 \cos\psi + \beta_2 \sin\psi$
β_o	Coning angle
β_1	Longitudinal tilt of tip path plane relative to horizontal reference plane
β_{1_s}	Longitudinal tilt of tip path plane relative to shaft $= \beta_1 + \vartheta_f - \xi_s$
β_2	Lateral tilt of tip path plane relative to horizontal reference plane

*These are moving axes, passing through the c.g. and rotating with the body.

γ	Lock number $= c\rho aR^4/I_b$
δ	Rotor vertical advance ratio $= \dot{z}/\Omega R$ where z = vertical displacement of rotor hub from space fixed origin
$\theta_{s\psi}$	Blade pitch angle at azimuth ψ, relative to shaft $= \theta_o + \theta_1 \sin\psi + \theta_2 \cos\psi$
θ_ψ	Blade pitch angle at azimuth ψ, relative to horizontal reference plane $= \theta_o + (\theta_1 - \alpha_1) \sin\psi + \theta_2 \cos\psi$
θ_o	Collective pitch at .75 radius
θ_1	Longitudinal cyclic pitch angle relative to shaft
θ_2	Lateral cyclic pitch angle relative to shaft
θ_f	Fuselage attitude angle, between $\bar{x}$-$\bar{x}$ axis and horizontal plane, positive nose up
λ	Initial inflow relative to tip path plane, positive down
μ	Rotor advance ratio $= \dot{x}/\Omega R$, where x = horizontal displacement of rotor hub from space fixed origin
ξ_s	Forward tilt of rotor shaft with respect to $\bar{z}$-$\bar{z}$ axis
ρ	Air mass density
σ	Rotor solidity $= bc/\pi R$
ϕ	Roll angle
Φ_f	$= \tan^{-1}\left(\frac{V_i}{\mu\Omega R}\right)$
Φ_t	$= \tan^{-1}\left(\frac{V_{i_t}}{\mu\Omega R}\right)$
ψ	Blade azimuth angle / Helicopter yaw angle — Context should clarify intended usage
Ω	Rotor rotational speed

Subscripts:

o	trim condition
fus, f	fuselage
mr	main rotor
tr	tail rotor
vt	vertical tail
t	horizontal stabilizer
TT	tip-mounted engine nacelle

Stability Derivatives:

Dimensionless stability derivatives referred to horizontal and vertical axes (origin at hub, blade flapping degree of freedom included):

$$x_\mu,\quad x_{\alpha_1},\quad x_{\hat{\alpha}_1},\quad x_\delta,\quad x_{\hat{\beta}_1},\quad x_{\beta_1},\quad x_{\theta_1},\quad z_\mu,\quad z_{\alpha_1},\quad z_\delta,$$

$$z_{\hat{\beta}_1},\quad z_{\beta_1},\quad z_{\theta_1},\quad m_\mu,\quad m_{\alpha_1},\quad m_{\hat{\alpha}_1},\quad m_\delta,\quad m_{\hat{\beta}_1},\quad m_{\beta_1},\quad m_{\theta_1},$$

$$\beta_{1_\mu},\quad \beta_{1_{\alpha_1}},\quad \beta_{1_\delta},\quad \beta_{1_{\hat{\beta}_1}},\quad \beta_{1_{\theta_1}}$$

where:

$$x_\mu = \frac{\partial\left(\frac{X}{m\,\Omega_o^2 R}\right)}{\partial \mu}\ ,\ \text{etc.}$$

$$z_\mu = \frac{\partial\left(\frac{Z}{m\,\Omega_o^2 R}\right)}{\partial \mu}\ ,\ \text{etc.}$$

$$m_\mu = \frac{\partial\left(\frac{M}{I_{yy}\,\Omega^2}\right)}{\partial \mu}\ ,\ \text{etc.}$$

$$\beta_{1_\mu} = \frac{\partial \beta_1}{\partial \mu}\ ,\ \text{etc.}$$

ANGULAR NOMENCLATURE

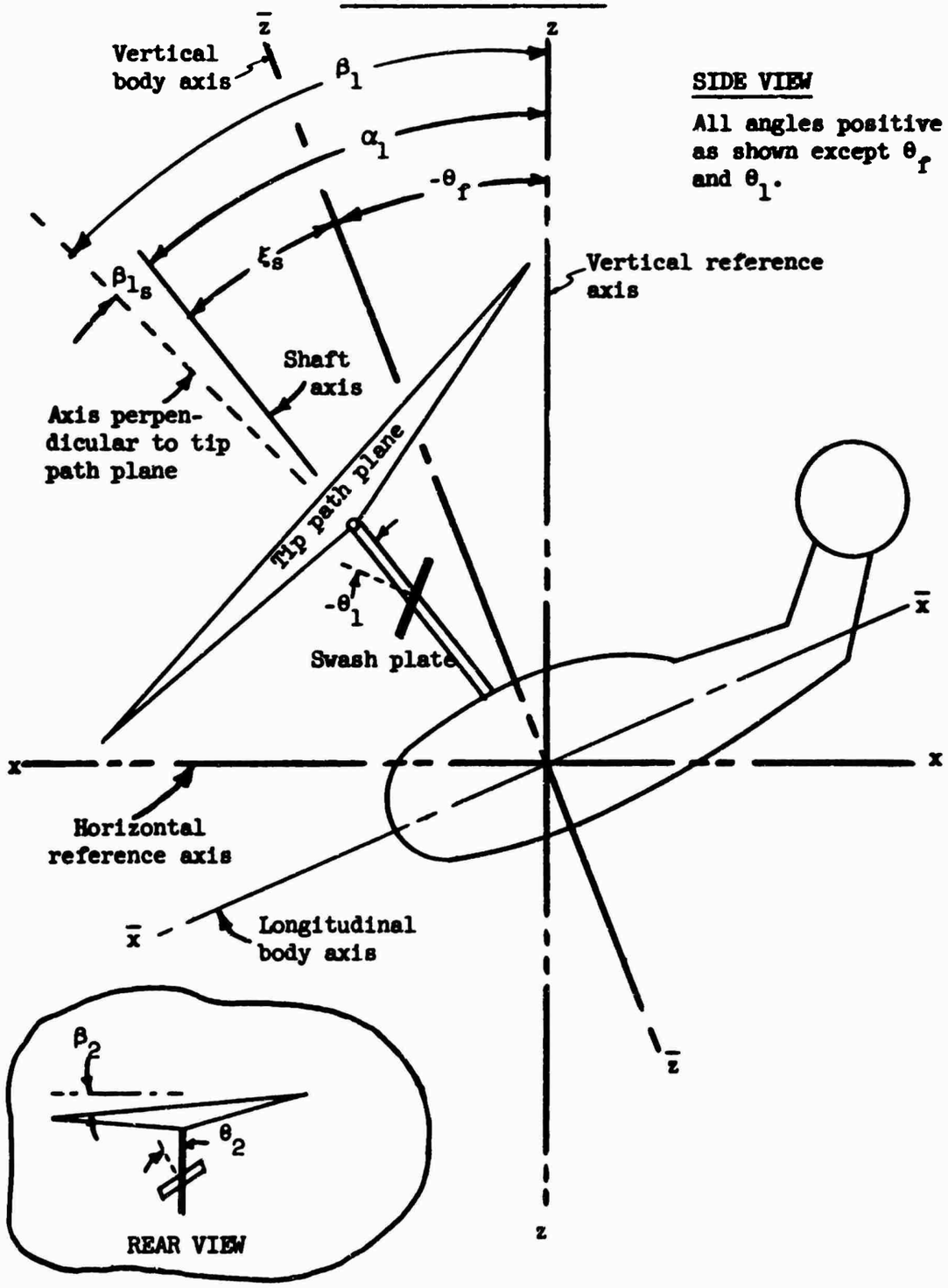

1.0 SUMMARY

The purpose of the analysis reported herein was to evaluate the feasibility of the tip turbo concept from a stability and control standpoint. A crane configuration fuselage was mated to the Model 1108 rotor system as a model for analysis. This helicopter configuration was not intended as an optimum design, but as a realistic configuration suitable for evaluating the flying characteristics. This configuration was evaluated from hover to 108-1/2 knots for both the design gross weight and the return mission gross weight.

The Military Specification for Helicopter Flying Qualities (MIL-H-8501A) was used as a guide for stability and control criteria. Specific items checked against this specification were: control position and body attitude as a function of forward speed; body attitude response at hover; maneuver response at hover and forward speed; response to artificial disturbance at forward speed; and stick-fixed dynamics. All of these requirements were met or exceeded. In many cases the Model 1108 was compared to additional criteria, other than MIL-H-8501A, which were felt to be more applicable to a heavy lift helicopter. Control power criteria, used as a design objective for this report, far exceeds the requirements of MIL-H-8501A.

All of the analysis is shown for the helicopter configuration alone, with no addition of stability augmentation. While augmentation is not required to satisfy the criteria, it is shown that augmentation will be required to achieve preferred handling qualities.

2.0 CONCLUSIONS

The tip turbo concept is feasible from a stability and control standpoint. This feasibility is based on comparison of the Model 1108 characteristics with the requirements of MIL-H-8501A, as well as more stringent criteria when it was felt to be more applicable.

The control power criteria of MIL-H-8501A is not adequate for helicopters of the Model 1108 weight class. A more applicable criteria is based on flight test studies of helicopter angular acceleration due to control input. These studies (reported in NASA TN D-58, Reference 8) indicate desirable levels of control power to be two to three times that required by MIL-H-8501A.

3.0 DISCUSSION

3.1 Longitudinal Stability and Control

3.1.1 Longitudinal Trim Conditions

The Model 1108 has adequate control power to provide trimmed, level flight over the desired speed range. A reasonable body attitude is maintained at all speeds, and sufficient margin of control is available for maneuvering.

Longitudinal cyclic position and fuselage attitude are shown in Figure 3 for level forward flight. The curves are smooth, with no objectionable reversal in slope.

The incidence angle of the horizontal stabilizer and forward tilt of the rotor mast were adjusted to provide a balance between two requirements: (1) reasonable fuselage attitude over the desired speed range; and (2) sufficient margin of control travel throughout the speed range to provide at least 10 percent of the maximum available pitching moment in hovering. Figure 3 shows these requirements to be satisfied. The most critical condition for control margin is trimmed level flight at maximum speed, with the aft center of gravity loading. Two degrees of control travel are available beyond trim at this flight condition. This provides a margin of 20 percent of the available control in hovering.

The slope of the cyclic control position is stable over the desired speed range for the normal gross weight. The light gross weight has a stable slope, except for a small region of neutral stability from hover to 20 knots forward. A stable slope is defined when a rearward displacement of the cyclic stick is required to hold a decreased value of steady forward speed, and a forward displacement is required to hold an increased value of speed.

Control force stability with respect to speed follows as a consequence of the control position stability. Control forces at the pilot's stick will be proportional to stick displacement. An irreversible actuator system will be used to obtain blade pitch, and a spring system will provide a positive force gradient to the pilot's stick.

A spring restraint system has been included in the main rotor design to restrain the main rotor in flapping. This design feature has been added to achieve desirable handling qualities. It was assumed that the spring restraint would have little effect on longitudinal trim conditions. The dynamic analysis of this report is based on the trim conditions of Figure 3 (which do not include the effect of the spring restraint). A calculation of the effect of the spring restraint substantiates this assumption. The effect of spring restraint on fuselage attitude is shown on the following page.

The difference in fuselage attitude due to spring restraint does not exceed 1 degree over the entire speed range. This difference may easily be balanced by a small change in stabilizer incidence angle, if desired.

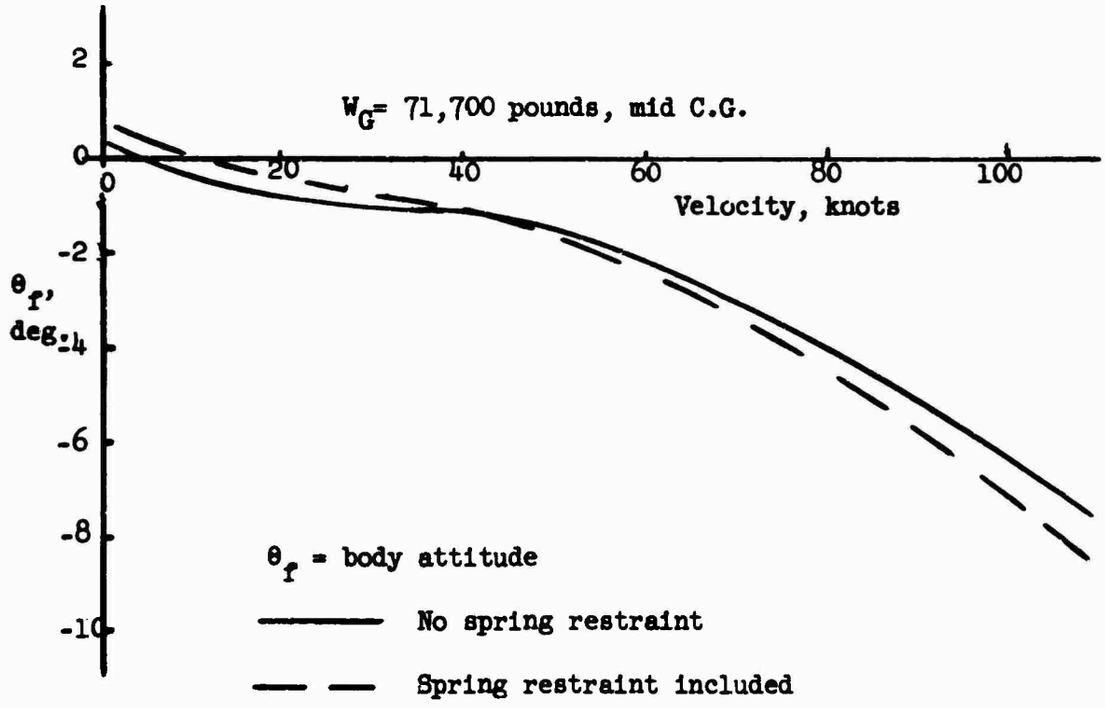

Figure 1. Effect of Spring Restraint on Trim Attitude.

3.1.2 Dynamic Stability and Control

3.1.2.1 Response to Control Input

3.1.2.1.1 Attitude Response at Hover

The response to control input has been designed to provide desirable handling qualities. In order to achieve the desirable characteristics, it was necessary to include a spring system to restrain the flapping motion of the main rotor blades. A spring restraint of 374,000 foot-pounds per radian per blade was found adequate. This amount of spring restraint is equivalent to a flapping hinge offset of 1-1/2 percent of blade radius. The resulting design provides attitude response characteristics which exceed the requirements of MIL-H-8501A (Reference 1). The control power criteria, used as the design objective, is discussed in Section 5.5.

Table 1 compares the Model 1108 response with the requirements of Reference 1. The response to control input was obtained by calculating the inverse of the transfer function, $\alpha_1(s)/\theta_1(s)$. This analytical procedure,

in addition to an analysis of the effect of spring restraint, is discussed in Section 5.3.4. The angular displacements, listed in Table 1, are in response to a step control input as defined below.

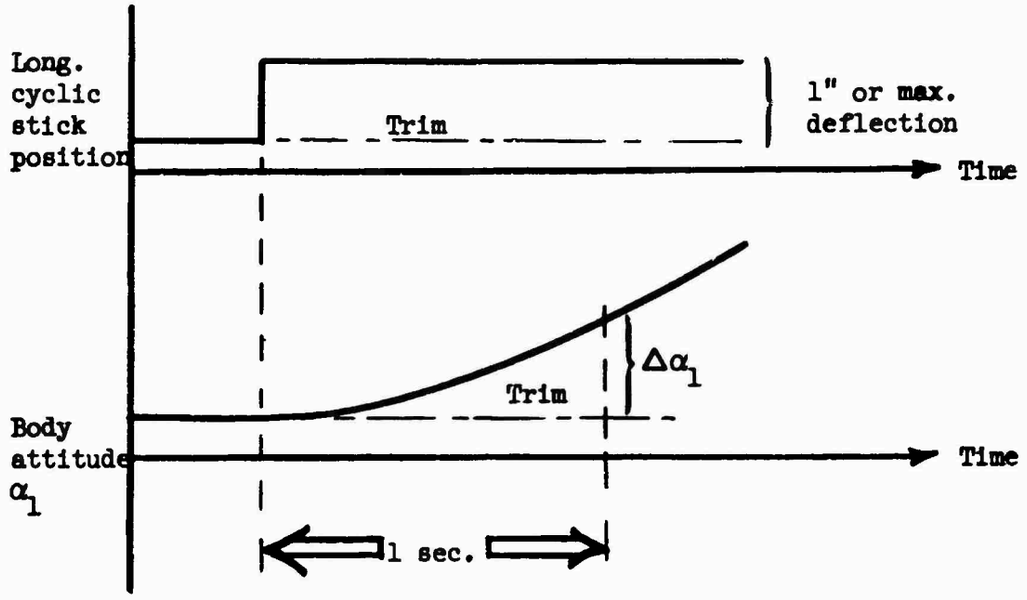

Figure 2. Longitudinal Control Response.

TABLE 1
PITCH ATTITUDE RESPONSE
(HOVER IN STILL AIR, SEA LEVEL, MID c.g.)

Gross Weight (lb)	Longitudinal Cyclic Stick Input	Angular Displacement in Pitch at the End of One Second	
		Model 1108 $\Delta\alpha_1$, Deg.	MIL-H-8501A Requirement $\Delta\alpha_1$, Deg.
39,200	One inch displacement from trim.	4.6	1.3 $\Delta\alpha_1 = \frac{45}{\sqrt[3]{W_G+1000}}$
71,700		4.6	1.1
*71,700		5.6	1.1
39,200	Maximum displacement from trim.	26.8	5.2 $\Delta\alpha_1 = \frac{180}{\sqrt[3]{W_G+1000}}$
71,700		26.7	4.3
*71,700		32.1	4.3

*Load suspended from c.g. by sling. (All other conditions have rigidly attached load.)

3.1.2.1.2 Maneuver Control at Hover and Forward Speed

The Model 1108 satisfies the maneuver requirements of Reference 1. These maneuver requirements are quoted below:

Reference 1, Paragraph 3.2.11.1:

a) Normal acceleration stipulation. Applies to speeds above that for minimum power required.

"After the longitudinal control stick is suddenly displaced rearward from trim a sufficient distance to generate a 0.2 radian/sec. pitching rate within 2 seconds, or a sufficient distance to develop a normal acceleration of 1.5g within 3 seconds, or 1 inch, whichever is less, and then held fixed, the time-history of normal acceleration shall become concave downward within 2 seconds following the start of the maneuver, and remain concave downward until the attainment of maximum acceleration. Preferably, the time-history of normal acceleration shall be concave downward throughout the period between the start of the maneuver and the attainment of maximum acceleration."

b) Angular velocity stipulation. Applies to all forward speeds, including hovering.

"During this maneuver, the time-history of angular velocity shall become concave downward within 2.0 seconds following the start of the maneuver, and remain concave downward until the attainment of maximum angular velocity; with the exception that for this purpose, a faired curve may be drawn through any oscillations in angular velocity not in themselves objectionable to the pilot. Preferably, the time-history of angular velocity should be distinctly concave downward throughout the period between 0.2 second after the start of the maneuver and the attainment of maximum angular velocity."

Time histories of longitudinal maneuvers are presented in Figure 4 for the normal gross weight and center of gravity. These time histories were obtained from the analog computer setup described in Section 5.3.5. Longitudinal control inputs of .92 inches for hover and 1.0 inch for forward speed are the minimum control inputs satisfying paragraph 3.2.11.1 (a and b), Reference 1. The points of inflection for the normal acceleration time histories occur within 1-1/2 seconds or less from the start of each maneuver. The point of inflection for the angular velocity occurs within 1/2 second or less from the start of each maneuver. These maneuver characteristics satisfy the required portion of paragraph 3.2.11.1, Reference 1, and approach the preferable response.

The preceding discussion demonstrates compliance with military specification requirements for pitch attitude response and maneuver characteristics.

An additional check on the maneuverability is desirable. As a heavy lift crane configuration, the Model 1108 may be called upon for precise positioning over a fixed ground reference, or for landing in a minimum of cleared area. Military missions will demand a minimum of time required to accomplish a pick up or delivery. Unprepared or hastily prepared sites, and adverse wind conditions must be considered. These conditions make the need for precise horizontal control very apparent. The capability of the Model 1108 for precise horizontal control is compared below with a proposed maneuver criteria.

As an index of horizontal control, Mr. Robert R. Lynn of Bell Helicopter Company, has proposed the following maneuver criterion (Reference 2). The proposed maneuver is a horizontal acceleration from hover defined as follows:

> "From a hover, at maximum gross weight with full adverse trim (c.g.) with a wind velocity of V_g from the critical direction, while maintaining the initial altitude, develop a steady state translational acceleration of $n_{x,y}$ within t seconds from the start of the maneuver. A curve of translational acceleration as a function of time shall have no abrupt slope changes. During the maneuver, a control margin of 10 percent of the total control travel shall be maintained and equal magnitude input and recovery control displacements will be used."

The following definitions apply to the above maneuver:

a) The time interval, t = 1.5 seconds. (This was selected as the maximum time duration that may be associated with the evaluation of initial response.)

b) V_g = 30 f.p.s.

c) The applied control input is 3/4 of the available control deflection, to allow for real and not step inputs.

Reference 2 presents calculated values of the translational acceleration capabilities of some existing helicopters (HU-1A, HU-1B, 47J, S-58, and S-64), for the above maneuver. The calculated results may be summarized as follows:

a) A longitudinal acceleration (n_x) of 0.15g is a representative value for the assumed maneuver. (Since the helicopters considered are acceptable for general use from the standpoint of maneuverability, 0.15 g may be considered as a valid lower level for hovering maneuverability.)

b) Although the calculated values show some scatter, the longitudinal acceleration capability did not appear to be a function of aircraft size.

The Model 1108 was subjected to the same control input as the above proposed maneuver for a comparison of horizontal control. The magnitude of control input was calculated as follows:

Flight condition: $W_G = 71{,}700$ lb., aft c.g.
Sea level, hover.

Limit of longitudinal cyclic travel,	$\theta_1 = 12^\circ$
Less θ_1 required to trim 30 f.p.s. wind,	-2°
	10°
Less 10 percent margin	-1°
Available θ_1 for maneuver	9°

θ_1 input = 3/4(9) = 6.75 degrees, .118 radian

Figure 5 shows an analog computer time history of horizontal acceleration, following a control reversal input of this magnitude. A horizontal acceleration of over 0.3g is achieved in the required time interval. This preliminary investigation indicates that the Model 1108 will be able to perform precise hovering at least as well as the existing helicopters compared in Reference 2.

3.1.2.2 Response to Artificial Disturbance

The response of the Model 1108 to an artificial disturbance indicates that the pilot should have adequate time for corrective action following an attitude disturbance. The MIL-H-8501A requirement for response to attitude disturbance is quoted below:

Paragraph 3.2.11.2, Reference 1:

> "To insure that a pilot has reasonable time for corrective action following moderate deviations from trim attitude (as, for example, owing to a gust), the effect of an artificial disturbance shall be determined. When the longitudinal control stick is suddenly displaced rearward from the trim, the distance determined in 3.2.11.1 above, and held for at least 0.5 second, and then returned to and held at the initial trim position, the normal acceleration shall not increase by more than 0.25g within 10 seconds from the start of the disturbance, except 0.25g may be exceeded during the period of control application. Further, during the subsequent nose down motion (with the controls still fixed at trim) any acceleration drop below the trim value shall not exceed 0.25g within 10 seconds after passing through the initial trim value."

Analog computer time histories of the response to an artificial disturbance are presented on Figure 6. The control stick has been displaced 1 inch aft, corresponding to the requirements of Section 3.1.2.1.2. The

maximum deviation of normal acceleration from trim is 0.2g, or less, for both flight conditions. This satisfies the requirements of Reference 1.

3.1.2.3 Stick-Fixed Dynamics

The longitudinal stick-fixed dynamics satisfy the requirements of Reference 1 without the aid of stability augmentation. Some stability augmentation will be required to achieve desirable handling qualities beyond the basic requirements of Reference 1. The need for stability augmentation is more fully discussed in the sections on lateral-directional dynamics (3.2.2), and control power and damping criteria (5.5). It should be emphasized that the requirements of Reference 1 are very adequately met by the stability of the basic configuration, but augmentation will be required to achieve preferred flying qualities.

The dynamic behavior has been determined by examining the roots of the characteristic equation of the longitudinal dynamics. The procedure for obtaining the characteristic equation is described in Section 5.3.4. Table 2 presents the roots of the characteristic equation, plus the time and number of cycles to double or half amplitude. The requirements of Reference 1 are included for comparison. The modes of motion are presented for hover, maximum speed, and an intermediate speed, for both the light and fully loaded gross weights. The data is presented for the nominal center of gravity, with the addition of one aft center of gravity point for comparison. All of the short period and aperiodic roots are well damped. The long period roots are either lightly damped or slowly divergent. Reference 1 allows some divergence for the long period roots, if the time to double amplitude is greater than 10 seconds. The time to double amplitude for the divergent roots far exceeds this requirement.

The modes of motion are more graphically presented as time histories on Figure 7. The stick-fixed response to an initial displacement of body attitude from trim is shown for the fully loaded gross weight. The same initial disturbance was used for all three speeds to provide a uniform basis for comparison. These time histories were obtained on the analog computer circuit described in Section 5.3.5. The long period mode is the predominant mode for all three flight conditions. The short period and aperiodic modes are so well damped that they do not appear in the transient response.

TABLE 2
STICK-FIXED LONGITUDINAL DYNAMICS
(LEVEL FLIGHT AT SEA LEVEL)

Gross Weight	c.g.	Velocity	Roots $\lambda = n \pm i\omega$		Period	$t_{\frac{1}{2}x}$	t_{2x}	$c_{\frac{1}{2}x}$	c_{2x}	MIL-H-8501A, Par. 3.2.11 Requirement
(lb)		(knots)	n	ω	Sec.	Sec.	Sec.			
39,200	Mid	0	.007447	.24073	26.1	-	93.2	-	3.57	$t_{2x} > 10$ sec.
			-2.2901	.55050	11.4	.303	-	.0265	-	$t_{2x} > 10$ sec.
			-2.6415	-	-	.262	-	-	-	Not Applicable
		60.0	-.008086	.18576	33.8	85.7	-	2.53	-	$t_{2x} > 10$ sec.
			-2.1908	1.7540	3.58	.316	-	.0883	-	$c_{\frac{1}{2}x} \leq 2$
			-2.3580	-	-	.294	-	-	-	Not Applicable
		108.5	.009900	.24984	25.1	-	70.0	-	2.78	$t_{2x} > 10$ sec.
			-2.0445	1.7398	3.61	.339	-	.0939	-	$c_{\frac{1}{2}x} \leq 2$
			-2.8544	-	-	.243	-	-	-	Not Applicable
71,700	Mid	0	.043170	.32118	19.6	-	16.0	-	.821	$t_{2x} > 10$ sec.
			-1.2484	-	-	.555	-	-	-	Not Applicable
			-1.4440	-	-	.480	-	-	-	Not Applicable
			-3.4094	-	-	.203	-	-	-	Not Applicable
		60.0	.006123	.24570	25.6	-	113.2	-	4.43	$t_{2x} > 10$ sec.
			-2.1166	1.3000	4.83	.328	-	.0678	-	$c_{\frac{1}{2}x} \leq 2$
			-1.3648	-	-	.508	-	-	-	Not Applicable
		108.5	.001235	.24541	25.6	-	561.2	-	21.9	$t_{2x} > 10$ sec.
			-1.5531	1.4159	4.44	.446	-	.1006	-	$c_{\frac{1}{2}x} \leq 2$
			-2.5022	-	-	.277	-	-	-	Not Applicable
71,700	Aft	108.5	-.00949	.2331	26.9	73.0	-	2.71	-	$t_{2x} > 10$ sec.
			-1.6294	1.7934	3.50	.425	-	.125	-	$c_{\frac{1}{2}x} \leq 2$
			-2.3631	-	-	.293	-	-	-	Not Applicable

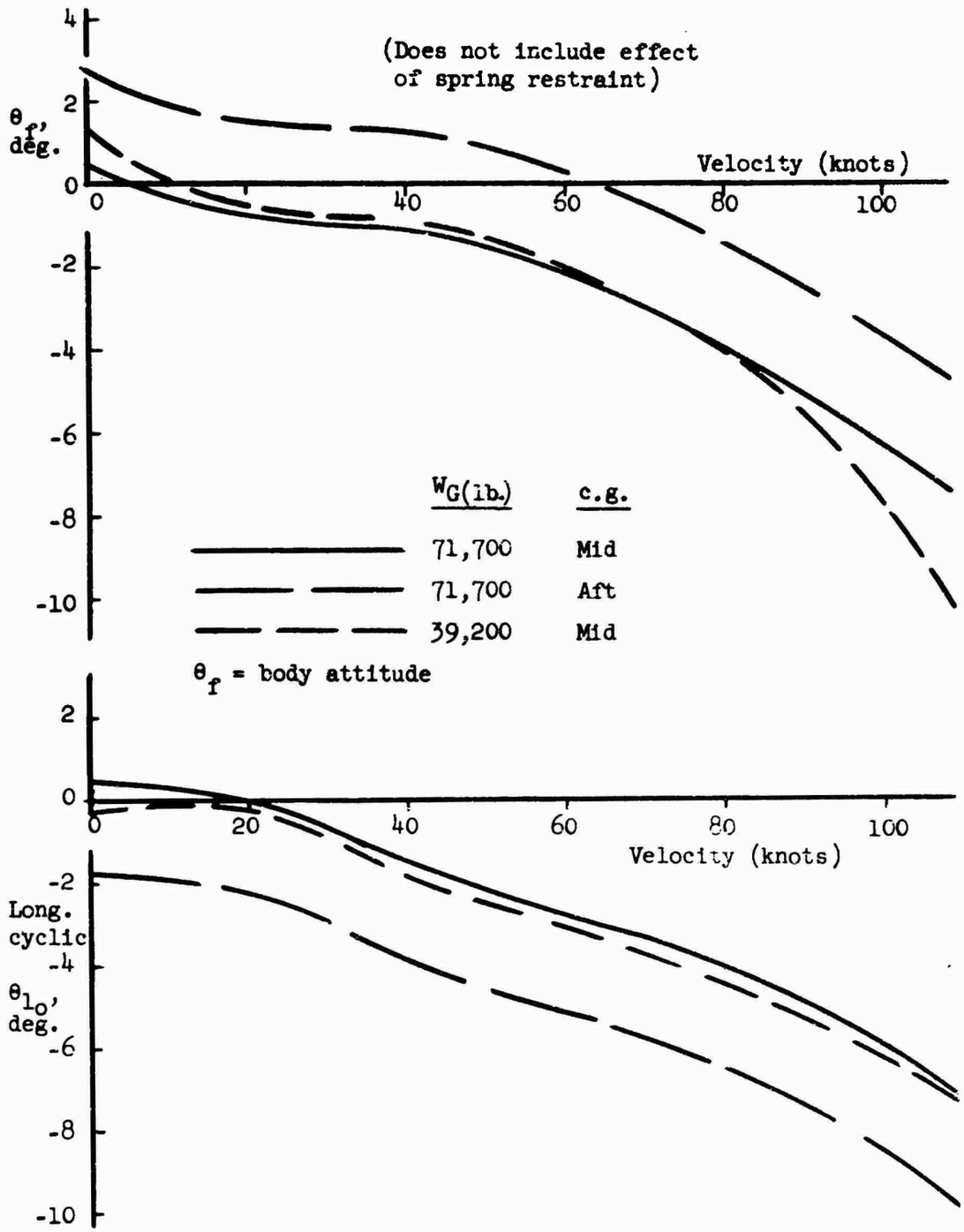

Figure 3. Longitudinal Trim Conditions.

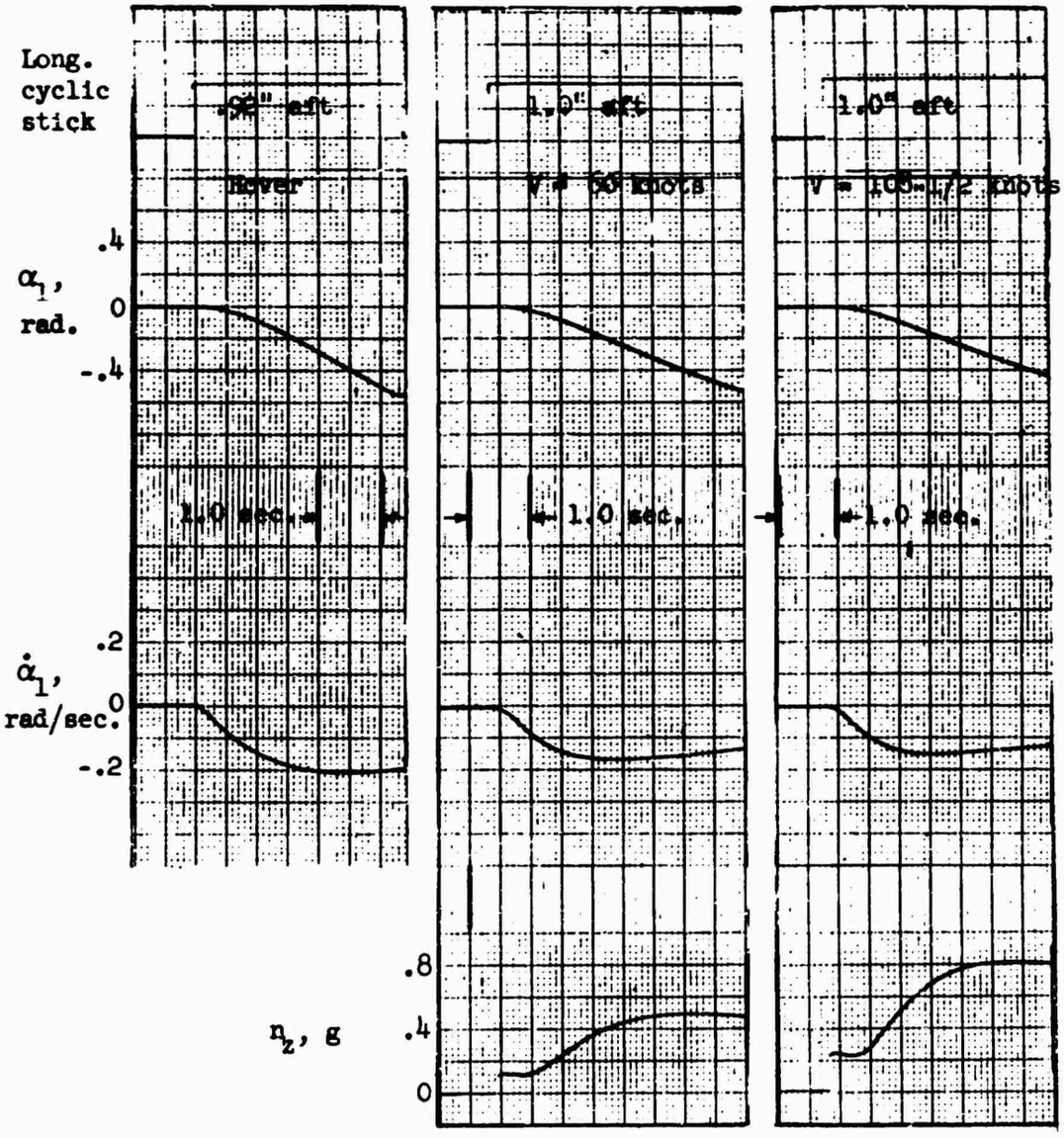

Figure 4. Longitudinal Maneuver Stability.
W_G = 71,700 pounds, Mid c.g.

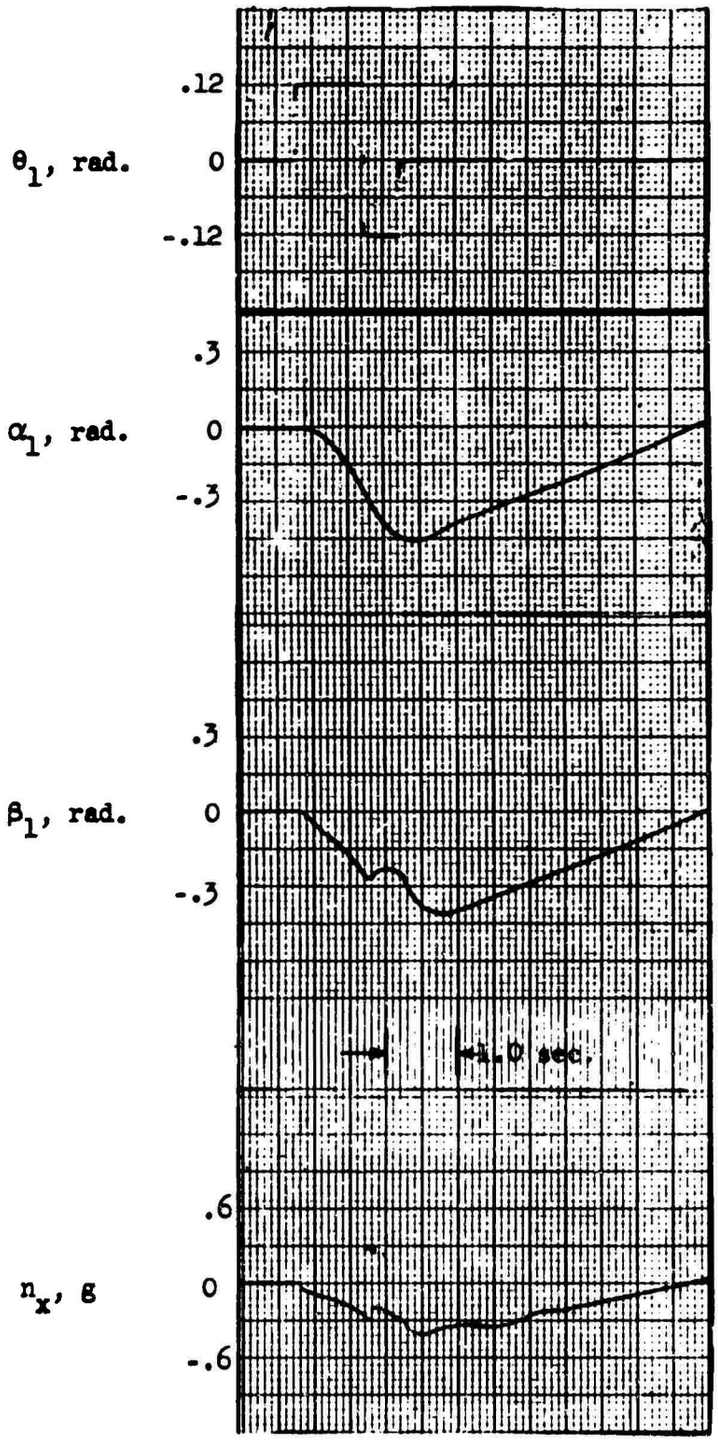

Figure 5. Horizontal Control at Hover.
W_G = 71,700 pounds, Mid c.g.

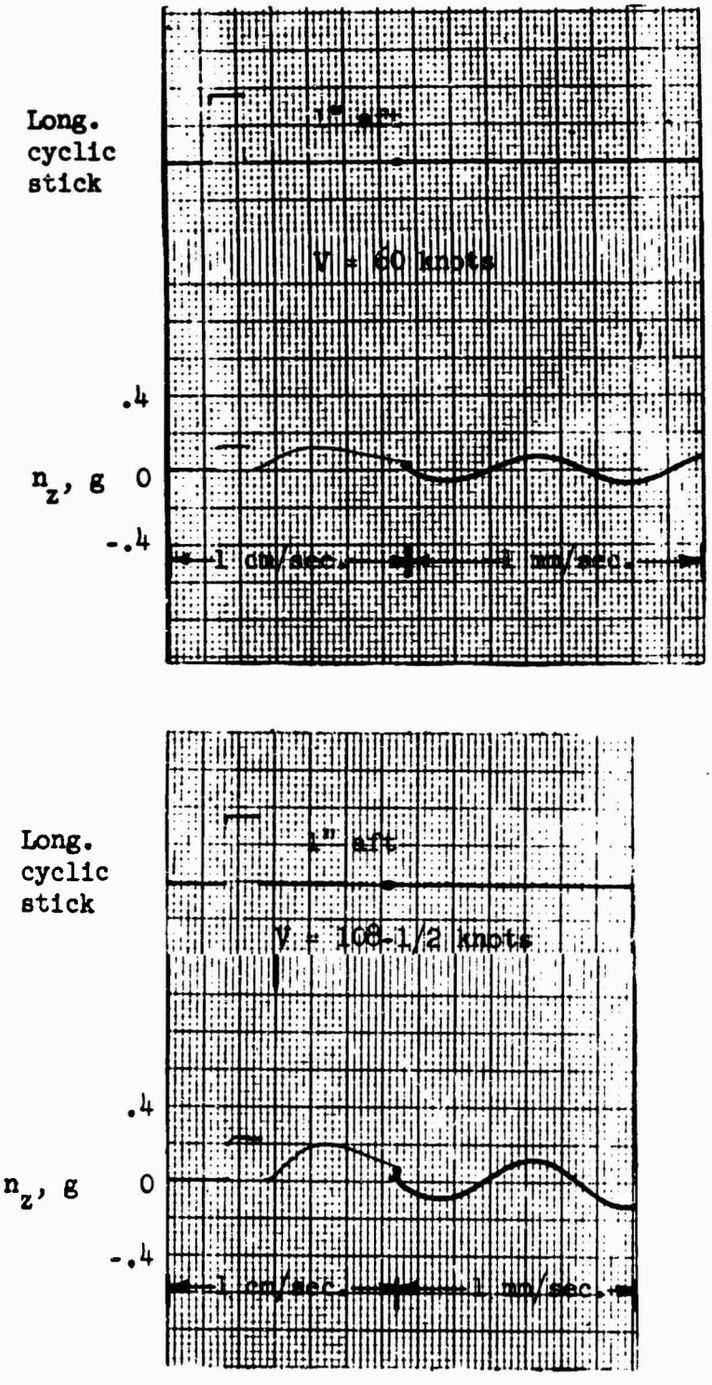

Figure 6. Longitudinal Response to Artificial Disturbance.
W_G = 71,700 pounds, Mid c.g.

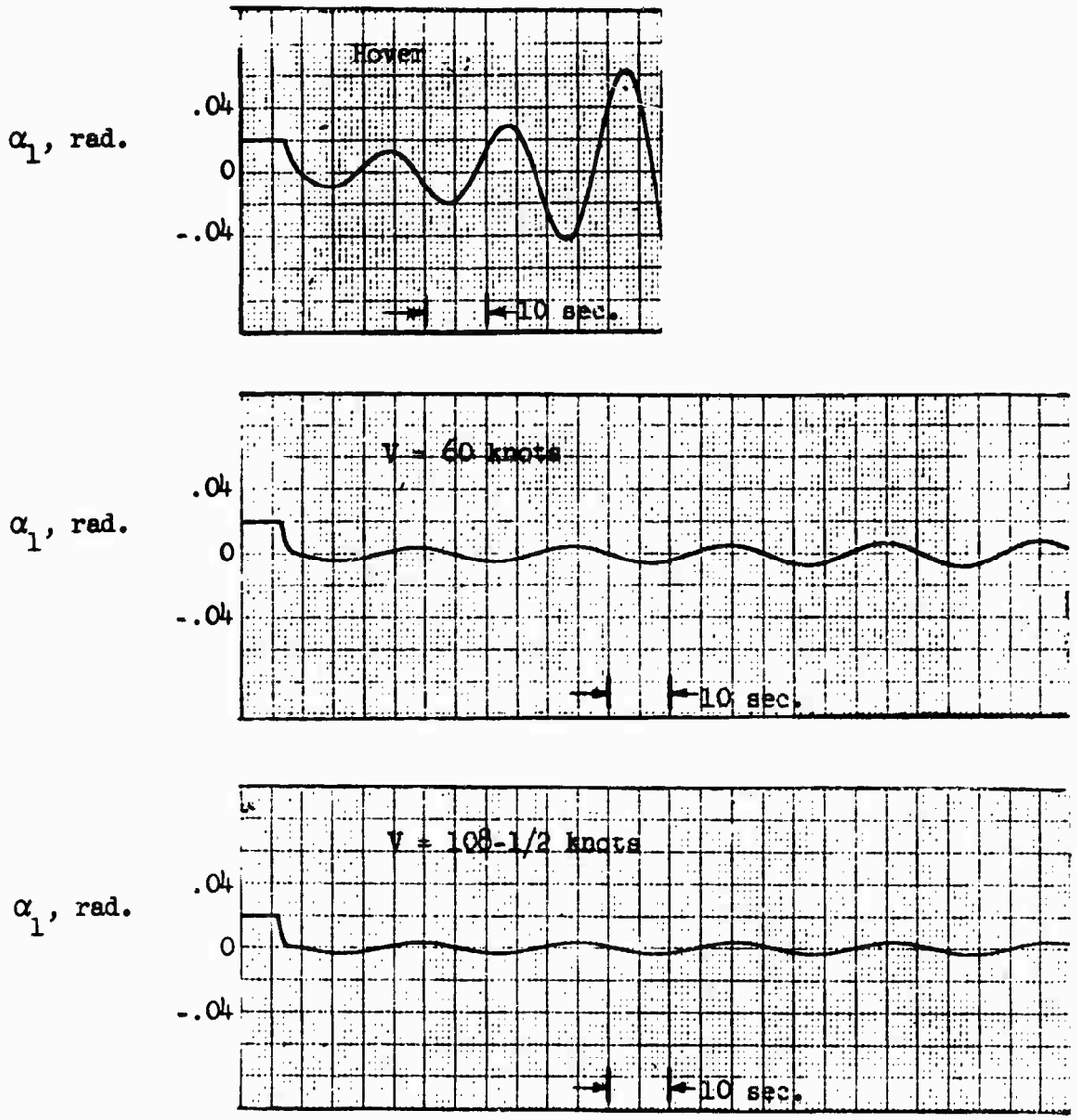

Figure 7. Longitudinal Stick-Fixed Time History.
W_G = 71,700 pounds, Mid c.g.

3.2 Lateral-Directional Stability and Control

3.2.1 Response to Control Input

3.2.1.1 Roll Response at Hover

The roll angle response in hover is similar to the pitch attitude response in hover. The spring restraint system affects the roll and pitch axes equally, except for the difference in fuselage inertias. Table 3 compares the Model 1108 roll response with the requirements of MIL-H-8501A, Reference 1. The roll angle displacements, listed in this table, are in response to the control input sketched below. (Note the difference in time interval between the roll and pitch response requirements.) The method of calculation of this response is discussed in Section 5.4.1.

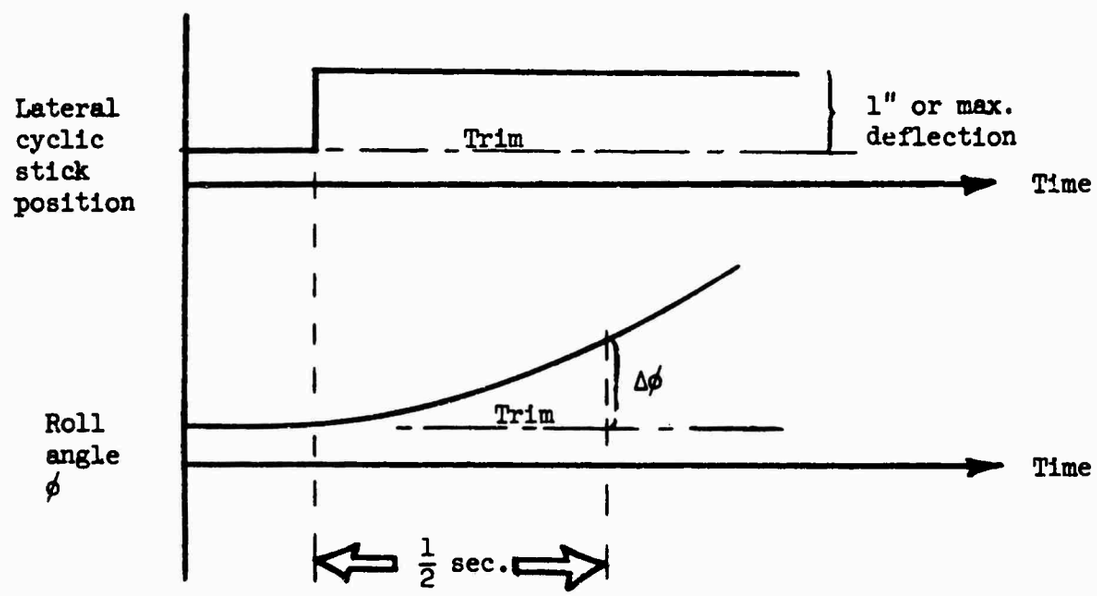

Figure 8. Lateral Control Input.

TABLE 3
ROLL ANGLE RESPONSE
(HOVER IN STILL AIR, SEA LEVEL, MID C.G.)

Gross Weight (lb)	Lateral Cyclic Stick Input	Angular Displacement in Roll at the End of 1/2 Second		
		Model 1108 $\Delta\phi$, Deg.	MIL-H-8501A Requirement $\Delta\phi$, Deg.	
39,200	One-inch	1.8	0.8	$\Delta\phi = \frac{27}{\sqrt[3]{W_G+1000}}$
71,700	displacement	1.4	0.6	
*71,700	from trim.	2.1	0.6	
39,200	Maximum	10.6	2.4	$\Delta\phi = \frac{81}{\sqrt[3]{W_G+1000}}$
71,700	displacement	8.5	1.9	
*71,700	from trim.	12.4	1.9	

*Load suspended from c.g. by sling. (All other conditions have rigidly attached load.)

3.2.1.2 Directional Response at Hover

The yaw angle developed after one second of step rudder pedal input is given in Table 4 below. The change in yaw angle required by MIL-H-8501A, Reference 1, is also indicated. The required yaw angle is achieved for each condition, although the response for one-inch pedal input is marginal.

TABLE 4
YAW ANGLE RESPONSE
GROSS WEIGHT = 71,700 LB.

Rudder Pedal Input	Wind Condition	Angular Displacement in Yaw at the End of 1 Second		
		Model 1108 $\Delta\psi$, Deg.	MIL-H-8501A Requirement $\Delta\psi$, Deg.	
Full left pedal	No wind.	-11.8	-7.9	$\Delta\psi = \frac{330}{\sqrt[3]{W_G+1000}}$
" " "	35-knot wind from right.	-4.3	-2.6	$\Delta\psi = \frac{110}{\sqrt[3]{W_G+1000}}$
1 inch left	No wind.	-2.9	-2.6	
Full right pedal	No wind.	10.3	7.9	$\Delta\psi = \frac{330}{\sqrt[3]{W_G+1000}}$
" " "	35-knot wind from left.	3.2	2.6	$\Delta\psi = \frac{110}{\sqrt[3]{W_G+1000}}$
1 inch right	No wind.	2.4	2.6	

The yaw angle response is not symmetrical for left and right pedal inputs. This nonlinearity exists for the following reasons:

a) Steady tail rotor thrust, at zero rudder pedal deflection, must balance main rotor bearing friction and torque for main rotor-driven accessories.

b) Tail rotor thrust is a nonlinear function of tail rotor collective pitch due to the effect of inflow velocity.

The above two effects are illustrated on Figure 9. The increment in tail rotor thrust available for control (indicated by ΔT_{tr} on Figure 9) is shown for hovering in still air and with a 35-knot crosswind. Increased rudder pedal deflection is required to hover in a crosswind to offset the increased tail rotor inflow angle.

Main rotor downwash was included in calculating the tail rotor thrust curve of Figure 9. This accounts for the thrust curve not becoming asymptotic at zero collective pitch. This beneficial effect of the main rotor downwash will be reduced at lighter gross weights. Good yaw response for small control inputs can be assured by designing the tail rotors with some steady opposing thrust.

3.2.2 Stick-Fixed Dynamics

The lateral-directional behavior has been determined in the same manner as classical fixed-wing airplane stability. Three degrees of freedom have been considered: roll, yaw, and sideslip. The lateral-directional equations of motion used in this report are provided in Section 5.4.1. The equations of motion combine to form a fourth order characteristic equation of the lateral-directional dynamics. The roots of this equation correspond to the following modes of motion:

Hover:
a) Long-period roll oscillation
b) Aperiodic yaw mode
c) Aperiodic roll mode

Forward speed:
a) Dutch-roll oscillation
b) Aperiodic spiral mode
c) Aperiodic roll mode

The characteristics of these modes are presented in Table 5 for the light and normal gross weight loadings. The speed range is covered by three flight conditions. All of the conditions are for the mid center-of-gravity loading. The aft center-of-gravity loading is also shown at maximum speed for comparison. Table 5 shows all of the modes to be stable, except for the long-period hover mode for the fully loaded gross weight. Each mode is more fully discussed in the text following the table.

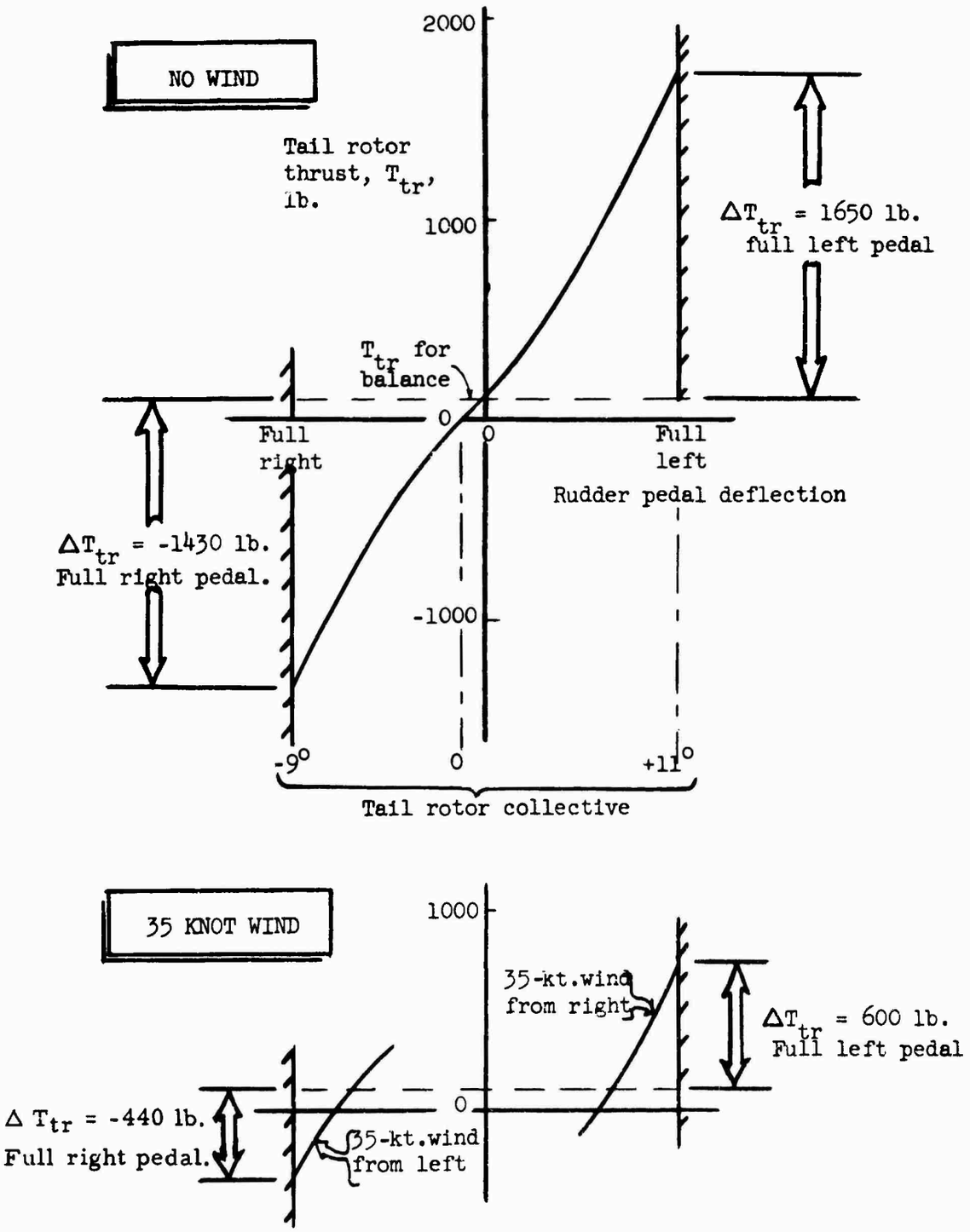

Figure 9. Tail Rotor Thrust for Control.
(Gross weight = 71,700 pounds.)

TABLE 5
STICK-FIXED LATERAL-DIRECTIONAL DYNAMICS
LEVEL FLIGHT AT SEA LEVEL

Gross Weight	c.g.	Velocity	Root $\lambda = n \pm i\omega$		Period	$t_{\frac{1}{2}x}$	t_{2_x}	$c_{\frac{1}{2}x}$	c_{2_x}	Mode
(lb)		(knots)	n	ω	sec.	sec.	sec.			
↑ 39,200 ↓	↑ Mid ↓	0	-.002788	.24303	25.8	248.6	-	9.62	-	*Long period roll oscil.
			-1.3149	-	-	.527	-	-	-	Yaw
			-2.0643	-	-	.336	-	-	-	Roll
		60.0	-.62680	1.6481	3.81	1.11	-	.2901	-	Dutch roll
			-.017015	-	-	40.7	-	-	-	Spiral
			-2.6521	-	-	.261	-	-	-	Roll
		108.5	-.62947	2.2074	2.85	1.10	-	.3869	-	Dutch roll
			-.072840	-	-	9.52	-	-	-	Spiral
			-1.7792	-	-	.390	-	-	-	Roll
↑ 71,700 ↓	↑ Mid ↓	0	.033484	.32883	19.1	-	20.7	-	1.084	*Long period roll oscil.
			-.80469	-	-	.861	-	-	-	Yaw
			-1.1843	-	-	.585	-	-	-	Roll
		60.0	-.40931	1.4103	4.46	1.69	-	.3801	-	Dutch roll
			-.021868	-	-	31.7	-	-	-	Spiral
			-1.6936	-	-	.409	-	-	-	Roll
		108.5	-.40671	1.8709	3.36	1.70	-	.5075	-	Dutch roll
			-.053909	-	-	12.8	-	-	-	Spiral
			-1.2212	-	-	.568	-	-	-	Roll
71,700	Aft	108.5	-.61601	2.2582	2.78	1.12	-	.4044	-	Dutch roll
			-.055667	-	-	12.4	-	-	-	Spiral
			-1.1713	-	-	.592	-	-	-	Roll

*These two roots obtained from longitudinal equations of motion by substituting roll inertia for pitch inertia. (All other roots obtained from lateral-directional equations of motion.)

Long-Period Roll Oscillation in Hover

This mode is the lateral counterpart to the long-period oscillation occurring in the longitudinal motion. As in the longitudinal case, it is a function of speed stability and angular velocity damping.

There is no direct military specification requirement for the damping of this mode. The requirement of paragraph 3.2.11, MIL-H-8501A (Reference 1) is the only related reference to dynamic characteristics. This requirement applies to longitudinal behavior in forward flight but may be considered applicable to the closely related roll mode. It states that for long-period oscillations (10- to 20-second periods), the oscillation may be divergent, but double amplitude shall not be achieved in less than 10 seconds.

Table 5 shows this motion to be lightly damped for the light gross weight. The motion is divergent for the fully loaded configuration but requires 20.7 seconds to achieve double amplitude. The behavior of the long-period hover oscillation therefore appears to be satisfactory.

Aperiodic Yaw Mode in Hover

This mode corresponds to the yaw rate damping in hover. Reference 1 has a specific requirement for this damping. Paragraph 3.3.19 of Reference 1 states: "The yaw angular velocity damping should preferably be at least $27(I_z)^{.7}$ ft.-lb./radian/sec." Table 6 compares the yaw damping for the Model 1108 with this requirement.

TABLE 6
YAW RATE DAMPING IN HOVER

Gross Weight	MIL-H-8501A Requirement		Model 1108
	$27(I_z)^{.7}$	$\frac{27(I_z)^{.7}}{I_z}$	
lb.	$\frac{\text{ft.-lb.}}{\text{rad./sec.}}$	Yaw Damping per Sec.	Yaw Damping per Sec.
39,200	74,100	.91	1.31
71,700	95,500	.81	.80

Aperiodic Roll Mode in Hover and Forward Speed

This mode corresponds to the roll rate damping. Reference 1 has a requirement for the amount of this damping in hover. The requirement for flight at forward speed is not specified. Table 7 shows these minimum requirements to be easily satisfied.

TABLE 7
ROLL RATE DAMPING

Gross Weight	Velocity	MIL-H-8501A Requirement		Model 1108
		$18(I_x)^{.7}$	$\frac{18(I_x)^{.7}}{I_x}$	
lb.	knots	$\frac{\text{ft.-lb.}}{\text{rad./sec.}}$	Roll Damping per Sec.	Roll Damping per Sec.
39,200	0	47,000	.62	2.06
↓	60.0	N.A.	N.A.	2.65
↓	108.5	N.A.	N.A.	1.78
71,700	0	85,000	.48	1.18
↓	60.0	N.A.	N.A.	1.69
↓	108.5	N.A.	N.A.	1.22

Spiral and Dutch-Roll Modes at Forward Speed

There is no requirement for the behavior of these modes in MIL-H-8501A, Reference 1. Reference 3 provides recommended requirements for lateral-directional handling qualities. These requirements are recommended for inclusion in military specifications for helicopters intended for instrument flight.

The requirements recommended by Reference 3, page 19, for dutch-roll and spiral mode behavior are as follows:

a) "At landing approach speeds and above, the lateral oscillation known as dutch-roll shall be well enough damped to lie on the favorable side of the acceptable-marginal boundary of 'Figure 5 herein.' It shall in no case be less than corresponds to half amplitude in two cycles."

b) "A spiral divergence shall in no case be stronger than corresponds to double amplitude in 7 seconds. Although convergence in this mode is desirable, slow divergence is permitted, provided the dutch-roll damping is sufficient."

The Model 1108 dutch-roll and spiral modes, listed in Table 5, are summarized below. The dutch-roll mode shows more damping than the minimum recommended requirement. The dutch-roll oscillation converges to half amplitude in well under 2 cycles. The spiral mode is stable at both speeds investigated.

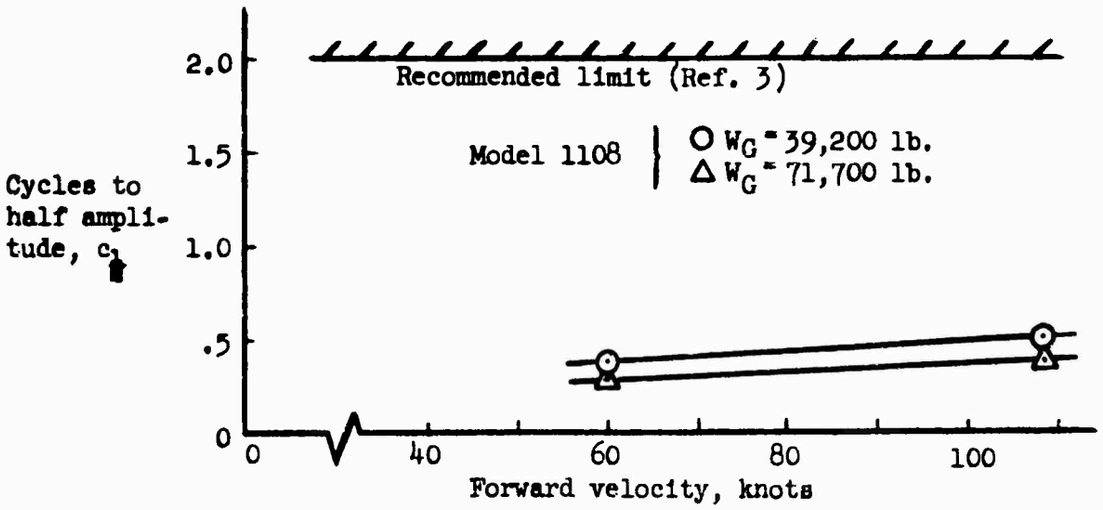

Figure 10. Dutch-Roll Mode.

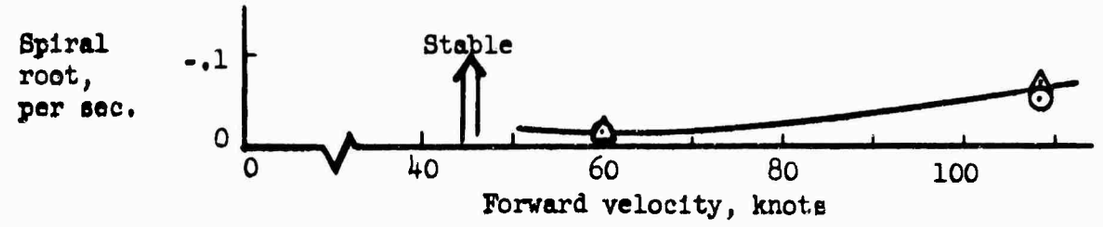

Figure 11. Spiral Mode.

The "Figure 5" referred to in item(a)on the preceding page applies to a configuration having greater roll damping than the Model 1108. Reference 3 shows desired dutch-roll and spiral characteristics to be a function of roll damping. The recommended dutch-roll and spiral characteristics for a degree of roll damping similar to the Model 1108 is more critical and is shown below.

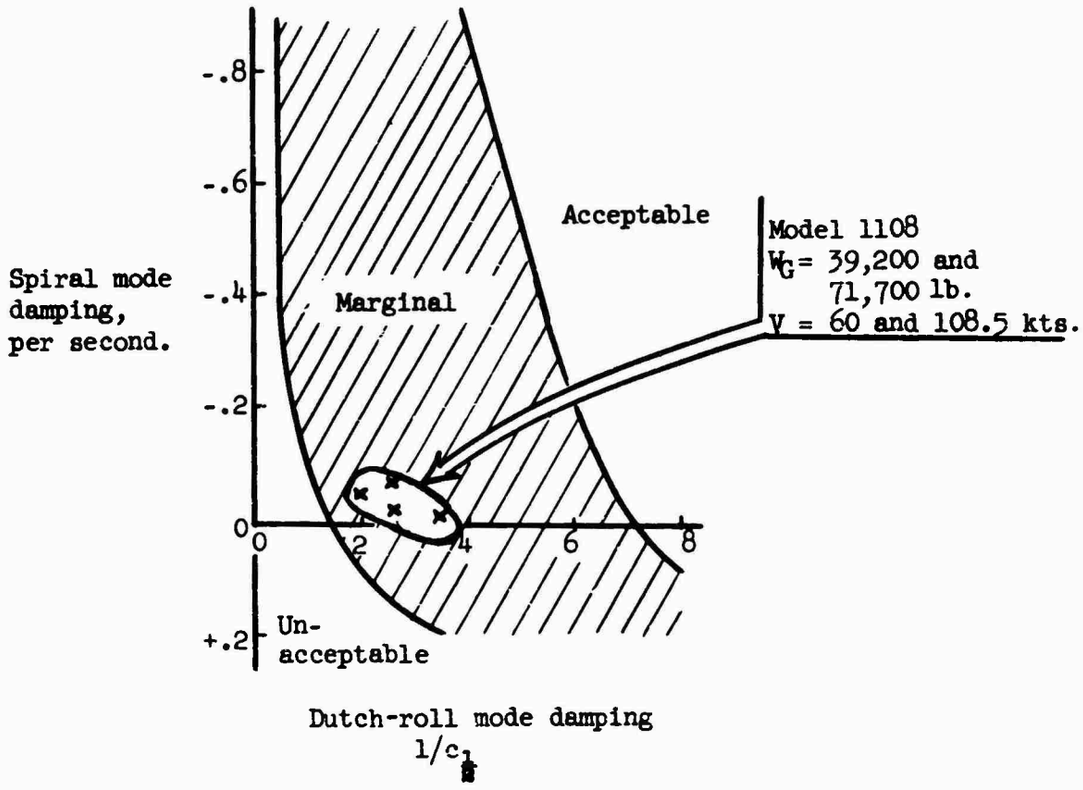

Figure 12. Lateral Handling-Qualities Boundaries.

(Roll damping = -2.67 per second)
Figure 6, Reference 3

Calculated values for the Model 1108 are within the "marginal" region of the recommended boundaries. It should be emphasized that the recommendations of Reference 3 apply to instrument flight, and should be interpreted in that context. The boundaries will be indicative of very desirable handling qualities. The "marginal" region is defined by Reference 3 as follows: "Considerable pilot effort required. Little attention could be given to other cockpit duties, such as radio, navigation, etc. Acceptable for flight in the event of stability augmentation device failing."

This illustrates the need for stability augmentation to provide good handling qualities. It also demonstrates that the basic configuration is flyable without augmentation. With sufficient control power to allow effective augmentation, the Model 1108 should exhibit good handling qualities.

4.0 REFERENCES

1. "Helicopter Flying and Ground Handling Qualities; General Requirements for," Military Specification MIL-H-8501A, September 7, 1961.

2. Lynn, Robert R., "New Control Criteria for VTOL Aircraft," Aerospace Engineering, Institute of the Aeronautical Sciences, New York, New York, August 1962.

3. Required Lateral Handling Qualities for Helicopters in Low-Speed Instrument Flight, TREC Report 60-66, Department of Aeronautical Engineering, Princeton University, Report No. 496, U. S. Army Transportation Research Command,* Fort Eustis, Virginia, February 1960.

4. Daughaday, DuWaldt, and Loewy, "Survey of Literature on Helicopter Stability and Derivation of Equations of Motion," Cornell Aero. Lab Report TB-707-S-2, Buffalo, New York, December 1954.

5. Dwinnell, James H., Principles of Aerodynamics, McGraw-Hill Book Company, New York, New York, 1949.

6. Perkins, Courtland D., and Hage, Robert E., Airplane Performance Stability and Control, John Wiley and Sons, Inc., New York, New York, 1953.

7. "Derivation of Lateral-Directional Equations of Motion," Hiller Aircraft Company Engineering Report No 64-14, Palo Alto, California, January 31, 1964.

8. Salmirs, Seymour, and Tapscott, Robert J., "The Effects of Various Combinations of Damping and Control Power on Helicopter Handling Qualities During Both Instrument and Visual Flight," NASA TN D-58, October 1959.

9. Faye, Alan E., Jr., "Additional Control Requirements for Hovering Determined Through the Use of a Piloted Flight Simulator," NASA TN D-792, April 1961.

10. Rolls, L. Stewart, and Drinkwater, Fred J., III, "A Flight Determination of the Attitude Control Power and Damping Requirements for a Visual Hovering Task in the Variable Stability and Control X-14A Research Vehicle," NASA TN D-1328, May 1962.

11. Amer, Kenneth B., "Theory of Helicopter Damping in Pitch or Roll and a Comparison With Flight Measurements," NACA TN 2136, October 1950.

---

*Changed to U. S. Army Aviation Materiel Laboratories in March 1965.

5.0 APPENDIX

5.1 Configuration Description

The stability and control analysis was based on the configuration shown on Figure 13. This configuration is not intended to be the optimum helicopter design for the Model 1108 rotor system. It was selected to provide a realistic configuration for stability and control analysis. The dimensions and characteristics are summarized below:

Main Rotor:

Airfoil section (constant)	0015
Chord (constant), ft.	6.5
Diameter, ft.	111.8
Number of blades	4
Solidity	0.148
Tip speed, ft/sec. - Hover	650
- Cruise	600
Twist, degrees	-10
Type	Teetering
Collective pitch movement degrees	15
Lateral cyclic movement, degrees	12
Longitudinal cyclic movement, degrees	12
Spring restraint per blade, ft-lb/rad.	374,000

Tail Rotors: (characteristics per rotor)

Chord (constant), ft.	0.98
Diameter, ft.	8.0
Moment arm, ft. (main rotor hub to tail rotor ℄)	38.0
Number of blades	5
Number of tail rotors (see Figure 14 for arrangement)	2
Solidity	0.39
Tip speed, ft/sec.	650
Twist, degrees	0
Collective pitch movement, degrees	+11,-9

Stabilizer:

Area, ft^2	48.0
Aspect ratio	3
Chord (constant), ft.	4.0
Incidence, degrees	0
Moment arm, ft. (main rotor hub to stabilizer quarter chord)	31.2
Span, ft.	12.0

Fuselage:

Equivalent flat plate area, $ft.^2$:	
Including cargo pod	200
Cargo pod removed	100

Tip Turbo Engines:

Inlet area, $ft.^2$ (both engines)	2.08
*Lift curve slope of nacelle, $(\partial C_L/\partial \alpha)_{TT}$ per rad.	4.5
Mounting	Over-Under
Number of engines per blade	2
*Profile drag, $C_{d_{TT}}$	$.282 + 4.125\alpha^2$

5.2 Mass Properties

Blade mass properties, per blade:

(including effect of engines at blade tip)

Mass, slugs	108.7
Distance of c.g. outboard of hub, ft.	29.4
Flapping moment of inertia about hub, $slug\text{-}ft.^2$	138,700

Helicopter mass properties:

(See Table 8.)

*Based on inlet area.

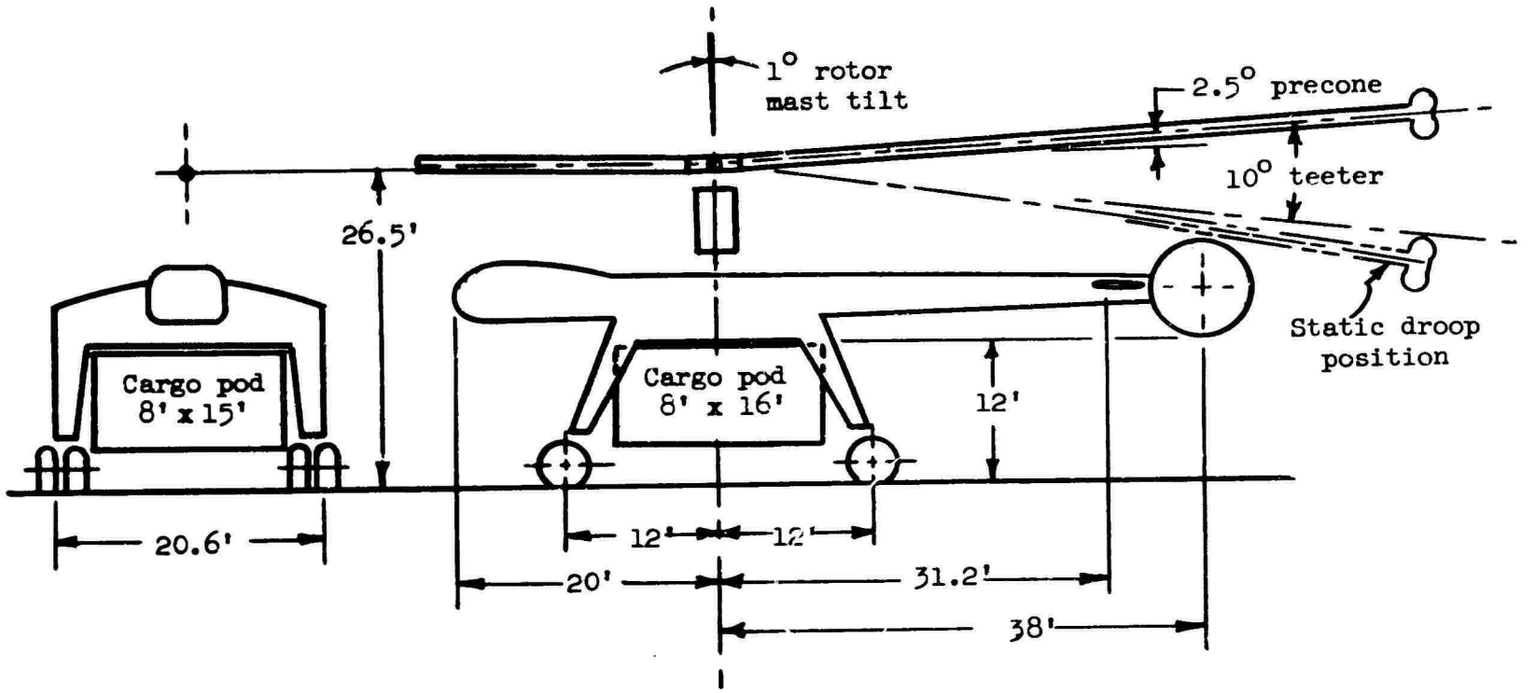

Figure 13. General Arrangement - Stability Analysis Model.

TABLE 8
HELICOPTER MASS PROPERTIES

Condition	Weight Breakdown				c.g.		Moments of Inertia			
	Gross	Empty + Crew	Fuel	Cargo	h	e_f	$I_{\bar{x}\bar{x}}$	$I_{\bar{y}\bar{y}}$	$I_{\bar{z}\bar{z}}$	$I_{\bar{x}\bar{z}}$
	(lb.)				(ft.)		(slug-ft^2)			
Light weight, no cargo	39,200	33,850	5,350	0	5.9	-.10	76,000	131,000	81,400	779.5
Fully loaded, rigid load, mid c.g.	71,700	33,850	13,850	24,000	10.9	-.06	178,000	228,000	117,500	-967.6
Fully loaded, rigid load, aft c.g.	71,700	33,850	13,850	24,000	10.9	-.50	178,000	189,500	78,900	-2770.2
Fully loaded, sling suspended load.	71,700	33,850	13,850	24,000	6.84	-.06	87,000	134,700	87,200	-610.1

e_f = distance of c.g. forward of main rotor hub.

h = distance of main rotor hub above c.g.

5.3 Longitudinal Analysis Methods

5.3.1 Main Rotor Trim Parameters

The main rotor trim parameters are presented in Table 9. These trim parameters have been calculated using an adaptation of the iterative method outlined on page 83 of Reference 4. The following six equations are iterated until a simultaneous set of solutions is obtained to within an accuracy of .01 percent between successive sets of solutions.

$$(\lambda_o)_{n+1} = \mu_o(\beta_{1_o})_n + V_{i_o}/\Omega R \tag{1}$$

$$(\theta_o)_{n+1} = \frac{\frac{4C_T}{\sigma a} + (\lambda_o)_{n+1} - \mu_o(\theta_{1_o} - \alpha_{1_o} + \beta_{1_o})_n}{\frac{2}{3} + \mu_o^2} \tag{2}$$

$$(\theta_{1_o} - \alpha_{1_o} + \beta_{1_o})_{n+1} = -\frac{16}{9}\mu_o\left[\frac{(\theta_o)_{n+1} - 3/4(\lambda_o)_{n+1}}{2/3 + \mu_o^2}\right] \tag{3}$$

$$(\beta_o)_{n+1} = \frac{\gamma}{2}\left[\frac{(\theta_o)_{n+1}(1 + \mu_o^2)}{4} + \frac{\mu_o}{3}(\theta_{1_o} - \alpha_{1_o} + \beta_{1_o})_{n+1} - \frac{(\lambda_o)_{n+1}}{3}\right] \tag{4}$$

$$(\beta_{2_o} - \theta_{2_o})_{n+1} = -\frac{4}{3}\left[\frac{\mu_o(\beta_o)_{n+1}}{1 + \mu_o^2/2}\right] \tag{5}$$

$$(\beta_{1_o})_{n+1} = \frac{\sigma a}{4C_T}\left\{\frac{C_{D_o}}{a}\mu_o + (\theta_o)_{n+1}\mu_o(\lambda_o)_{n+1} + \frac{(\lambda_o)_{n+1}}{2}(\theta_{1_o} - \alpha_{1_o} + \beta_{1_o})_{n+1} + \mu_o(\beta_o)_{n+1}^2\left[\frac{1}{2} - \frac{4}{9}\left(\frac{1}{1 + \mu_o^2/2}\right)\right]\right\} - \frac{C_{X_R}}{C_T} + \left\{\frac{n\rho(\Omega R)^2 S_{TT}\mu\left[C_{D_{TT}} + .51(\partial C_L/\partial\alpha)_{TT}\right]}{2W}\right\} \tag{6}$$

Iteration of Equations (1) through (6) was started using the following approximate expressions:

$$\lambda_o \sim \mu_o\left(-\frac{C_{X_R}}{C_T}\right) + \frac{V_{i_o}}{\Omega R}$$

$$\theta_o \sim \frac{4C_T/\sigma a + \lambda_o}{2/3 + \mu_o^2}$$

Induced velocity was calculated by the following formula:

$$V_{i_o} = \left\{ \frac{-(\Omega R\mu_o)^2 + \left[(\Omega R\mu_o)^4 + C_T^2 (\Omega R)^4\right]^{\frac{1}{2}}}{2} \right\}^{\frac{1}{2}}$$

The tip loss correction factor = 1.0 for the above equation.

Effect of Horizontal Force Due to Tip Turbo Nacelle Airloads:

Equations (1) through (6) are obtained by the method described on page 83 of Reference 4, with one exception. This exception is the last term of Equation (6), repeated below:

$$\left\{ \frac{n\rho(\Omega R)^2 S_{TT}\mu \left[\left(C_{D_{TT}} + .51 \left(\frac{\partial C_L}{\partial \alpha}\right)_{TT}\right]\right.}{2W_G} \right\}$$

The equations of Reference 4 are derived for a rotor blade free of discontinuities, and therefore do not account for the tip-mounted engine nacelle. An expression for the horizontal force due to the tip-mounted nacelles, Equation (19), is derived in Section 5.3.4. The change in tilt of the tip path plane, $\Delta\beta_{1_o}$, required to offset an increment of horizontal force is illustrated in the following vector diagram.

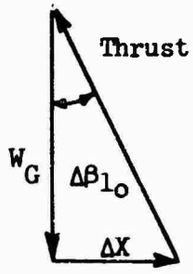

$$\Delta\beta_{1_o} \sim \frac{\Delta X}{W_G}$$

As an approximation we have

$$(\Delta\beta_{1_o})_{TT} = \frac{\Delta X_{TT}}{W_G}$$

From Section 5.3.4

$$\Delta X_{TT} = \frac{n}{2} \rho(\Omega R)^2 S_{TT}\mu \left[C_{D_{TT}} + .51 \left(\frac{\partial C_L}{\partial \alpha}\right)_{TT} \right] \qquad (19)$$

Finally,

$$(\Delta\beta_{1_o})_{TT} = \frac{n\rho(\Omega R)^2 S_{TT}\mu \left[C_{D_{TT}} + .51 \left(\frac{\partial C_L}{\partial \alpha}\right)_{TT} \right]}{2W_G}$$

This agrees with the last expression of Equation (6).

TABLE 9
MAIN ROTOR TRIM PARAMETERS

Gross Weight	c.g.	Velocity	V_i	λ_o	θ_o	β_o	β_{1_o}	$\theta_{1_o} - \alpha_{1_o}$	$\beta_{2_o} - \theta_{2_c}$
(lb.)		(knots)	(f.p.s.)		(radians)				
↑ 39,200 ↓	Mid	0	28.98	.0445781	.0949868	.0277071	0	0	0
		60.0	8.26	.0280995	.0780449	.0290436	.0848843	-.1094900	-.0064484
		108.5	4.58	.0838157	.1700073	.0334652	.2494367	-.3259896	-.0130205
↑ 71,700 ↓	Mid	0	39.19	.0602890	.1418666	.0479184	0	0	0
		60.0	14.99	.0358138	.1190782	.0512486	.0641138	-.1039430	-.0113785
		108.5	8.37	.0694356	.1814773	.0531359	.1816626	-.2741162	-.0206739
	*Mid	0	39.19	.062890	.1418666	.0479184	0	0	0
	Aft	108.5	8.37	.0694356	.1814773	.0531359	.1816626	-.2741162	-.0206739

*Load suspended from c.g. by sling.
(All other conditions have rigidly attached load.)

5.3.2 Fuselage Attitude Versus Forward Speed

Equation (11) was used to calculate trim fuselage attitude as a function of forward speed. The results of this calculation are plotted on Figure 3, page 11. The trim equation, plus the source of each term, is given below. The trim equation is derived at the end of this section, beginning on page 37.

$$\theta_f = \frac{W_G e_f + \hat{q}_o A_\pi h - \hat{q}_f SR\left[(C_{M_f})_{\alpha_f=0} - \left(\frac{\partial C_M}{\partial \alpha_f}\right)\Phi_f\right] + \hat{q}_t S_t \ell_t a_t (i_t - \Phi_t) + \frac{bk_\beta}{2}(\beta_i - \xi_s)}{-Wh + \hat{q}_o A_\pi e_f + \hat{q}_f SR\left(\frac{\partial C_M}{\partial \alpha_f}\right) - \hat{q}_t S_t \ell_t a_t - \frac{bk_\beta}{2}} \qquad (11)$$

where:

A_π = Fuselage equivalent flat plate area, ft^2

e_f = Distance of c.g. forward of main rotor hub, ft.

h = Distance of main rotor hub above c.g., ft.

i_t = Incidence angle of horizontal tail with respect to fuselage centerline (positive leading edge up), radians

ℓ_t = Distance of horizontal tail 1/4 chord aft of c.g., ft.

b = Number of rotor blades, main rotor

R = main rotor blade radius, ft.

S = πR^2, ft^2

S_t = Horizontal stabilizer area, ft^2

W_G = Helicopter gross weight, lb.

The above terms are all geometric and mass properties. These properties are tabulated in Sections 5.1 and 5.2 for each configuration considered. The remaining terms are given below.

a_t = Horizontal stabilizer lift curve slope, per radian

For aspect ratios, A, less than 6:

$$a_t = 2\pi\left(\frac{A}{A+3}\right), \text{ per radian} \quad \text{(page 145, Reference 5)}$$

$$A = 3$$

$$a_t = 2\pi(3/6) = 3.1416 \text{ per radian.}$$

For this analysis let $a_t = 3.0$ per radian.

$(C_{M_f})_{\alpha_f=0}$ = fuselage pitching moment coefficient at zero angle of attack, dimensionless.

Assume $(C_{M_f})_{\alpha_f=0} = 0$ for this analysis.

The fuselage contours are not adequately defined at this time to justify an approximation of this term. The value will be zero for a symmetrical fuselage.

$\frac{\partial C_M}{\partial \alpha_f}$ = rate of change of fuselage pitching moment with angle of attack, per radian.

$C_M = \frac{M}{qSR}$, by definition

where:

M = pitching moment, ft-lb.
q = dynamic pressure, p.s.f.
S and R defined above.

$$\frac{\partial C_M}{\partial \alpha_f} = \frac{\partial M / \partial \alpha_f}{qSR}$$

$$\frac{\partial M}{\partial \alpha} = \frac{q(K_2 - K_1)}{36.5} \int_o^{\ell} w_f^2 \, dx, \quad \text{ft-lb/deg.} \quad \text{(pg. 226, Ref.6)}$$

where:

$K_2 - K_1$ = fuselage correction for fineness ratio

$\sim .6$, for $L/D = \frac{56.5}{20.6} = 2.74$ (pg. 226, Ref. 6)

w_f = local fuselage width, ft.

dx = increment in fuselage length

The fuselage planform, used as a model for this analysis, is sketched on the following page.

Integrating the square of the width of this planform with respect to this length, we have

$$\int_o^{\ell} w_f^2 \, dx = 7386 \text{ ft}^3$$

Substituting in the equation of Reference 6,

$$\frac{\partial M}{\partial \alpha} = \frac{q(.6)(7386)}{36.5} \text{ , ft-lb/degree}$$

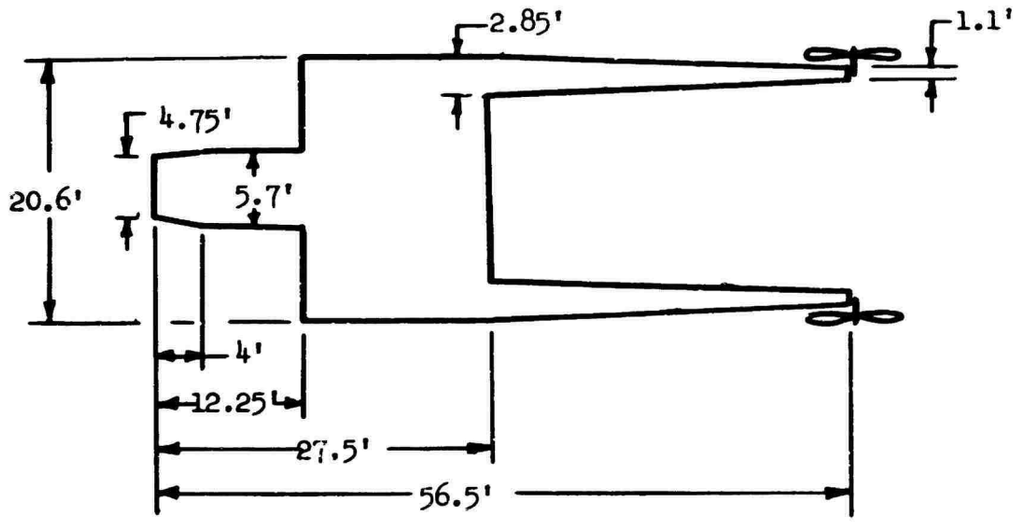

Figure 14. Planform Dimensions - Stability Analysis Model.

$$\frac{\partial C_M}{\partial \alpha_f} = \frac{\partial M/\partial \alpha}{qSR} = \frac{q(.6)(7386)(57.3)}{36.5(q)(SR)} \text{ , ft-lb/rad.}$$

R = 55.9

$$\frac{\partial C_M}{\partial \alpha_f} = \frac{.6(7386)(57.3)}{36.5(\pi)(55.9)^3} = .0127/\text{rad.}$$

Let $\frac{\partial C_M}{\partial \alpha_f} = .013/\text{rad.}$ for this analysis.

k_β = spring restraint per blade, ft-lb/rad.
= 374,000 lb-ft/rad. Note: This term was not included in the calculations for Figure 3, page 11. This spring effect was included for the comparison shown in Figure 1.

$$\hat{q}_o = \frac{1}{2}\rho(\mu\Omega R)^2 \text{ , p.s.f.}$$

$$\hat{q}_f = \frac{1}{2}\rho(\mu\Omega R)^2 + \frac{1}{2}\rho V_1^2 \text{ , p.s.f.}$$

$$\hat{q}_t = \frac{1}{2}\rho(\mu\Omega\delta)^2 + \frac{1}{2}\rho(V_1)_t^2 \text{ , p.s.f.}$$

$$\Phi_f = \tan^{-1}\left(\frac{V_1}{\mu\Omega R}\right)$$

$$\Phi_t = \tan^{-1}\left(\frac{V_{i_t}}{\mu\Omega R}\right)$$

V_i = induced velocity of main rotor, f.p.s. = $K_u \frac{1}{.97}\sqrt{\frac{W_G}{2\rho\pi R^2}}$

$(V_i)_t$ = induced velocity of main rotor at the horizontal stabilizer, f.p.s. = $1.414\left(\frac{\ell_t}{R}\right)V_i$

α_f = angle of attack of fuselage with respect to the relative wind, radians.

β_1 = longitudinal tilt of the tip path plane relative to the horizontal plane, radians. (This term calculated in Section 5.3.1.)

ξ_s = forward tilt of rotor shaft with respect to vertical body axis, radians, = 1/57.3 radians.

Derivation of Trim Fuselage Attitude as a Function of Forward Speed

This derivation is restricted to steady, level flight. Figure 15 serves as a simple model for analysis.

For trimmed, level flight:

$\Sigma F_z = 0$ (assuming L_t small)

$Z + W = 0, \quad Z = -W$

$\Sigma F_x = 0$ (assuming L_t small)

$X_{mr} + X_f = 0, \quad X_{mr} = -X_f$

$X_{mr} = -(1/2)(\rho)(\mu\Omega R)^2 A_\pi$

$\Sigma M_{cg} = 0$

$\Sigma M_{cg} = M_{mr} + M_f + M_t + M_{s_y} = 0$

where:

M_{cg} = pitching moment about c.g. (positive nose up)

M_{mr} = " " " " (due to main rotor)

M_f = " " " " (due to fuselage)

M_t = " " " " (due to horizontal tail)

M_{sy} = " " " " (due to spring restraint)

Each of these moment terms will now be derived.

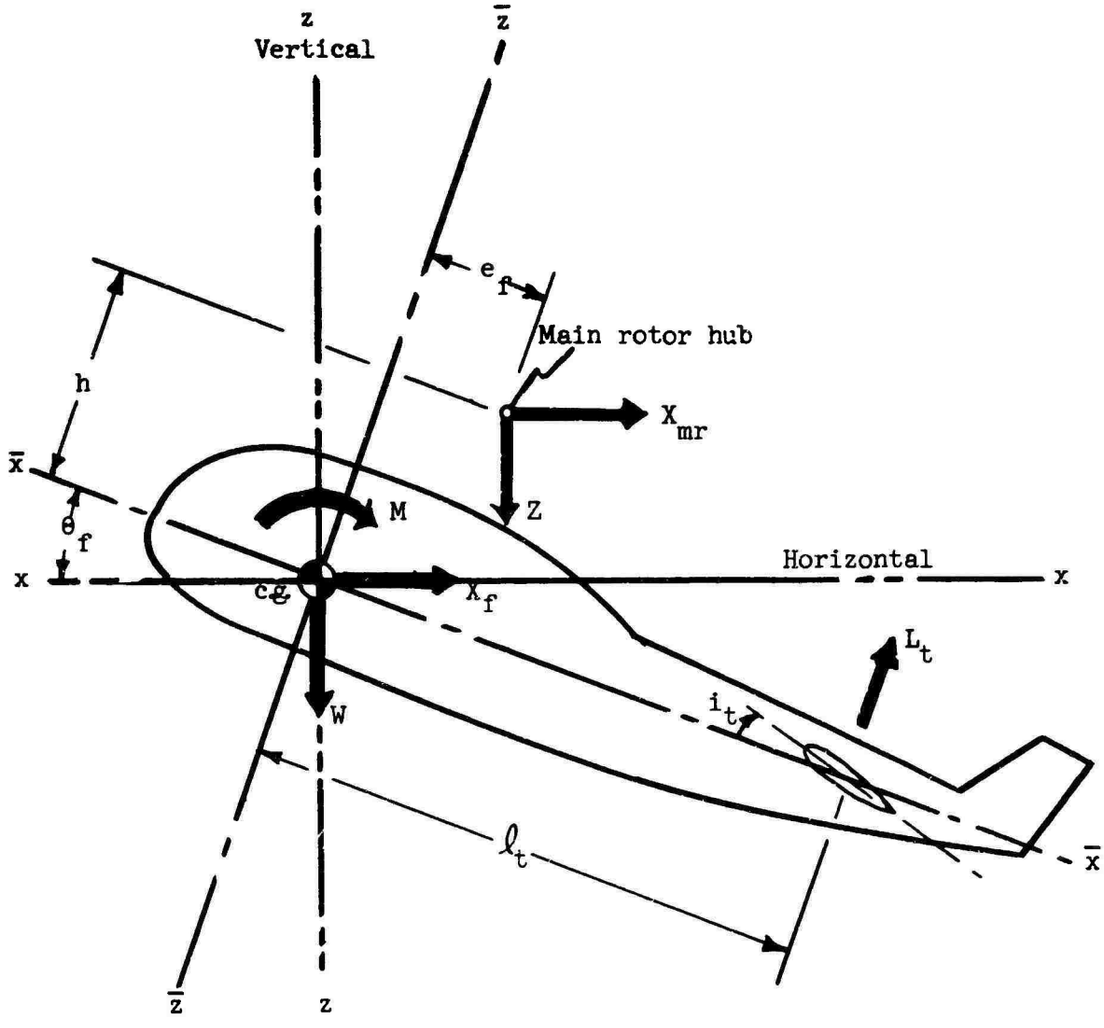

Figure 15. Forces and Moments for Trimmed Flight.

Moment Due to Main Rotor:

From inspection of Figure 15,

$$M_{mr} = Z(h \sin \theta_f + e_f \cos \theta_f) + X_{mr}(h \cos \theta_f - e_f \sin \theta_f)$$

where:

$$Z = -W_G$$

$$X_{mr} = -\frac{1}{2} \rho(\mu\Omega R)^2 A_\pi$$

$$\left.\begin{aligned} \sin \theta_f &= \theta_f, \text{ rad.} \\ \cos \theta_f &= 1 \end{aligned}\right\} \quad \text{assuming } \theta_f \text{ small}$$

Substituting:

$$M_{mr} = -W(h\theta_f + e_f) - \frac{1}{2} \rho(\mu\Omega R)^2 A_\pi (h - e_f\theta_f) \tag{7}$$

Moment Due to Fuselage:

$$M_f = \frac{1}{2} \rho U^2 (C_{M_f}) SR$$

where:

$$C_{M_f} = (C_{M_f})_{\alpha_f=0} + \frac{\partial C_M}{\partial \alpha_f} \alpha_f$$

$$\alpha_f = \theta_f - \tan^{-1} \frac{V_i}{\mu\Omega R}$$

$$U^2 = (\mu\Omega R)^2 + V_i^2$$

Substituting:

$$M_f = \frac{1}{2} \rho \left[(\mu\Omega R)^2 + V_i^2\right]\left[(C_{M_f})_{\alpha_f=0} + \frac{\partial C_M}{\partial \alpha_f} \left(\theta_f - \tan^{-1} \frac{V_i}{\mu\Omega R}\right)\right] SR \tag{8}$$

Moment Due to Horizontal Tail:

$$M_t = -\frac{1}{2} \rho U_t^2 C_{L_t} S_t \ell_t$$

where:

$$U_t^2 = (\mu\Omega R)^2 + (V_i)_t^2$$

$$C_{L_t} = a_t \alpha_t$$

$$\alpha_t = \theta_f + i_t - \tan^{-1} \frac{(V_i)_t}{\mu\Omega R}$$

Substituting:

$$M_t = -\frac{1}{2} \rho\left[(\mu\Omega R)^2 + (V_i)_t^2\right] a_t \left[\theta_f + i_t - \tan^{-1} \frac{(V_i)_t}{\mu\Omega R}\right] S_t \ell_t \tag{9}$$

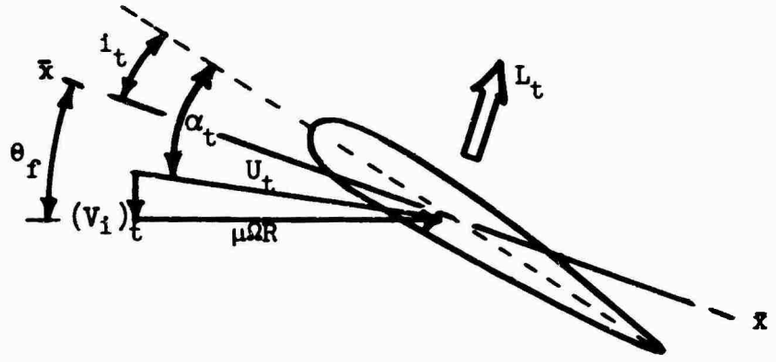

Figure 16. Angles and Forces on Horizontal Stabilizer.

Moment Due to Spring Restraint:

From Section 5.3.4:

$$M_{s_y} = \frac{bk_\beta(-\beta_{l_s})}{2} \tag{20}$$

But $$\beta_{l_s} = \theta_f + \beta_l - \xi_s$$

$$M_{s_y} = \frac{bk_\beta(-\theta_f - \beta_l + \xi_s)}{2} \tag{10}$$

Combining moment terms:

$$\Sigma M_{cg} = M_{mr} + M_f + M_t + M_{s_y} = 0$$

Substituting Equations (7) thru (10):

$$\Sigma M_{cg} = -W_G(h\theta_f + e_f) - \frac{1}{2}\rho(\mu\Omega R)^2 A_\pi(h - e_f\theta_f)$$
$$+ \frac{1}{2}\rho\left[(\mu\Omega R)^2 + V_i^2\right]\left[(C_{M_f})_{\alpha_f=0} + \frac{\partial C_M}{\partial \alpha_f}\left(\theta_f - \tan^{-1}\frac{V_i}{\mu\Omega R}\right)\right] SR$$
$$- \frac{1}{2}\rho\left[(\mu\Omega R)^2 + (V_i)_t^2\right] a_t\left[\theta_f + i_t - \tan^{-1}\frac{(V_i)_t}{\mu\Omega R}\right] S_t \ell_t$$
$$+ \frac{bk_\beta(-\theta_f - \beta_l + \xi_s)}{2} = 0$$

Expanding:

$$\Sigma M_{cg} = -W_G h\theta_f - W_G e_f - \frac{1}{2}\rho(\mu\Omega R)^2 A_\pi h + \frac{1}{2}\rho(\mu\Omega R)^2 A_\pi e_f \theta_f$$
$$+ \frac{1}{2}\rho\left[(\mu\Omega R)^2 + V_i^2\right](C_{M_f})_{\alpha_f=0} SR + \frac{1}{2}\rho\left[(\mu\Omega R)^2 + V_i^2\right]\frac{\partial C_M}{\partial \alpha_f}\theta_f SR$$
$$- \frac{1}{2}\rho\left[(\mu\Omega R)^2 + V_i^2\right]\frac{\partial C_M}{\partial \alpha_f}\left(\tan^{-1}\frac{V_i}{\mu\Omega R}\right) SR - \frac{1}{2}\rho\left[(\mu\Omega R)^2 + (V_i)_t^2\right] a_t \theta_f S_t \ell_t$$
$$- \frac{1}{2}\rho\left[(\mu\Omega R)^2 + (V_i)_t^2\right] a_t \left[i_t - \tan^{-1}\frac{(V_i)_t}{\mu\Omega R}\right] S_t \ell_t$$
$$- \left(\frac{bk_\beta}{2}\right)\theta_f - \left(\frac{bk_\beta}{2}\right)(\beta_1 - \xi_s) = 0$$

Introducing the following symbols for simplicity:

Let:
$$\hat{q}_o = \frac{1}{2}\rho(\mu\Omega R)^2$$
$$\hat{q}_f = \frac{1}{2}\rho(\mu\Omega R)^2 + \frac{1}{2}\rho V_i^2$$
$$\hat{q}_t = \frac{1}{2}\rho(\mu\Omega R)^2 + \frac{1}{2}\rho(V_i)_t^2$$
$$\Phi_f = \tan^{-1}\left(\frac{V_i}{\mu\Omega R}\right)$$
$$\Phi_t = \tan^{-1}\left(\frac{Vi_t}{\mu\Omega R}\right)$$

Substituting:

$$\Sigma M_{cg} = -W_G h\theta_f - W_G e_f - \hat{q}_o A_\pi h + \hat{q}_o A_\pi e_f \theta_f$$
$$+ \hat{q}_f SR(C_{M_f})_{\alpha_f=0} + \hat{q}_f SR\left(\frac{\partial C_M}{\partial \alpha_f}\right)\theta_f$$
$$- \hat{q}_f SR\left(\frac{\partial C_M}{\partial \alpha_f}\right)\Phi_f - \hat{q}_t S_t \ell_t a_t \theta_f$$
$$- \hat{q}_t S_t \ell_t a_t (i_t - \Phi_t) - \left(\frac{bk_\beta}{2}\right)\theta_f$$
$$- \left(\frac{bk_\beta}{2}\right)(\beta_1 - \xi_s) = 0$$

Solving for θ_f:

$$\theta_f = \frac{W_G e_f + \hat{q}_o A_\pi h - \hat{q}_f SR\left[(C_{M_f})_{\alpha_f=0} - \left(\frac{\partial C_M}{\partial \alpha_f}\right)\Phi_f\right] + \hat{q}_t S_t \ell_t a_t (i_t - \Phi_t) + \frac{bk_\beta}{2}(\beta_1 - \xi_s)}{-W_G h + \hat{q}_o A_\pi e_f + \hat{q}_f SR\left(\frac{\partial C_M}{\partial \alpha_f}\right) - \hat{q}_t S_t \ell_t a_t - \frac{bk_\beta}{2}} \qquad (11)$$

5.3.3 Longitudinal Stability Derivatives

Longitudinal stability derivatives are presented in Tables 10 through 12. These derivatives were calculated using the equations listed on pages 75 through 78 of Reference 4 and were based on a horizontal stabilizer having 2.18 times the effectiveness of the stabilizer used in the rest of this report, as the result of a calculation error. Increasing the stabilizer span by 70 percent will provide a corresponding effectiveness. This difference is felt to have little or no effect on the objective or conclusions of this study. At low speed there is no effect of the difference on the transient responses. At higher speed the difference would result in a small change in the response. It should be noted that all values are calculated and that in the normal course of helicopter design the tail would be sized from wind-tunnel and flight tests to achieve desired handling qualities. The equations of Reference 4 have been modified for the effects of the tip-mounted engine nacelles and main rotor spring restraint.

Effect of Tip-Mounted Engine Nacelles:

An expression for the horizontal force due to the tip-mounted nacelles, Equation (19), is derived in Section 5.3.4. We have,

$$\Delta X_{TT} = \frac{b}{2}\rho(\Omega R)^2 S_{TT}\mu\left[C_{D_{TT}} + .51\left(\frac{\partial C_L}{\partial \alpha}\right)_{TT}\right] \qquad (19)$$

By definition: $x_\mu = \dfrac{\partial X/\partial \mu}{m\Omega^2 R}$

Hence: $(\Delta x_\mu)_{TT} = \dfrac{\partial \Delta X_{TT}/\partial \mu}{m\Omega^2 R}$

$(\Delta x_\mu)_{TT}$ = effect of tip-mounted engine nacelle on longitudinal stability derivatives

Therefore: $(\Delta x_\mu)_{TT} = (b/2m\Omega^2 R)\rho\,(\Omega R)^2 S_{TT}\left[C_{D_{TT}} + .51(\partial C_L/\partial\alpha)_{TT}\right]$

This increment was added to the x_μ calculated using the equations of Reference 4.

Effect of Main Rotor Spring Restraint:

The equations of Reference 4 for the stability derivatives include the effect of a hinge offset, e. Section 5.3.4 shows the spring restraint to be related to an equivalent hinge offset, "e",

where $$\text{"e"} = k_\beta/m_b d\,\Omega^2 \qquad (21)$$

The effect of the spring restraint was included in calculation of stability derivatives by means of this equivalent hinge offset.

TABLE 10

LONGITUDINAL STABILITY DERIVATIVES
Gross Weight = 39,200 Pounds
Mid c.g., Sea Level

Forward Speed (knots)		0	60	108.5
x_μ		.0025117	.0055195	.0215033
	$x_{\hat{\alpha}_1}$	.0000000	-.0001944	-.0003516
x_{α_1}		-.0050632	.0000650	.0077843
	x_δ	.0000000	.0[illegible]799	.0597595
$x_{\hat{\beta}_1}$		.0000000	.0000309	.0001128
	x_{β_1}	.0008048	-.0017714	.0054715
x_{θ_1}		.0050632	-.0000650	-.0077843
z_μ		.0000000	.0188829	.0504656
	z_{α_1}	.0000000	.0383664	.0693731
z_δ		.2271550	.2271550	.2271550
	$z_{\hat{\beta}_1}$	.0000000	.0000000	.0000000
z_{β_1}		.0000000	.0000000	.0000000
	z_{θ_1}	.0000000	-.0383664	-.0693731
$\beta_{1\mu}$		-.1641466	-.1123670	-.0662821
	$\beta_{1\alpha_1}$	1.0000000	1.0578799	1.1956629
$\beta_{1\delta}$		.0000000	.3426879	.6406777
	$\beta_{1\hat{\beta}_1}$	-2.5660752	-2.6032063	-2.6915967
$\beta_{1\theta_1}$		-1.0000000	-1.0578799	-1.1956 29
m_μ		.0041051	.0054952	.0297749
	$m_{\hat{\alpha}_1}$	.0000000	.0120314	.0217549
m_{α_1}		.0396304	.0609617	.0538748
	m_δ	.0036308	.0350659	.0686160
$m_{\hat{\beta}_1}$		.0000000	.0000947	.0003452
	m_{β_1}	-.0396402	-.0550303	-.0328676
m_{θ_1}		.0155370	.0061085	.018[illegible]3

TABLE 11

LONGITUDINAL STABILITY DERIVATIVES
Gross Weight = 71,700 Pounds
Mid c.g., Sea Level

Forward Speed (knots)		0	60	108.5
x_μ		.0019342	.0039414	.0100029
	$x_{\hat{\alpha}_1}$	.0000000	-.0003929	-.0007104
x_{α_1}		-.0037437	-.0008788	.0025780
	x_o	.0000000	.0079864	.0237023
$x_{\hat{\beta}_1}$		.0000000	.0000298	.0000980
	x_{β_1}	-.0005147	-.0027704	-.0003363
x_{θ_1}		.0037437	.0008788	-.0025780
z_μ		.0000000	.0079127	.0202768
	z_{α_1}	.0000000	.0209758	.0379278
z_δ		.1241907	.1241907	.1241907
	$z_{\hat{\beta}_1}$	.0000000	.0000000	.0000000
z_{β_1}		.0000000	.0000000	.0000000
	z_{θ_1}	.0000000	-.0209758	-.0379278
β_{1_μ}		-.2577400	-.2070416	-.1567047
	$\beta_{1\alpha_1}$	1.0000000	1.0578799	1.1956629
$\beta_{1\delta}$		.0000000	.3426879	.6406777
	$\beta_{1\hat{\beta}_1}$	-2.5660752	-2.6032063	-2.6915967
$\beta_{1\theta_1}$		-1.0000000	-1.0578799	-1.1956629
m_μ		.0076850	.0061495	.0209889
	$m_{\hat{\alpha}_1}$	.0000000	.0069128	.0124995
m_{α_1}		.0273545	.0488799	.0468157
	m_δ	.0020601	.0230265	.0533608
$m_{\hat{\beta}_1}$		.0000000	.0001776	.0005833
	m_{β_1}	-.0273658	-.0449959	-.0305014
m_{θ_1}		.0222967	.0106077	.0154683

TABLE 12

LONGITUDINAL STABILITY DERIVATIVES
Miscellaneous Conditions
Gross Weight = 71,700 Pounds
Sea Level

Forward Speed (knots)		0	108.5
C.G.		Mid*	Aft
x_μ	$x_{\hat{\alpha}_1}$	.0019342 .0000000	.0100329 -.0007104
x_{α_1}	x_δ	-.0037437 .0000000	.0025780 .0237023
$x_{\hat{\beta}_1}$	x_{β_1}	.0000000 -.0005147	.0000980 -.0003363
x_{θ_1}		.0037437	-.0025780
z_μ	z_{α_1}	.0000000 .0000000	.0202768 .0379278
z_δ	$z_{\hat{\beta}_1}$	.1241907 .0000000	.1241907 .0000000
z_{β_1}	z_{θ_1}	.0000000 .0000000	.0000000 -.0379278
β_{1_μ}	$\beta_{1\alpha_1}$	-.2577400 1.0000000	-.1567047 1.1956629
$\beta_{1\delta}$	$\beta_{1\hat{\beta}_1}$	.0000000 -2.5660752	.6406777 -2.6915967
$\beta_{1\theta_1}$		-1.0000000	-1.1956629
m_μ	$m_{\hat{\alpha}_1}$	.0081635 .0000000	.0246085 .0150390
m_{α_1}	m_δ	.0443428 .0034865	.0581090 .0696630
$m_{\hat{\beta}_1}$	m_{β_1}	.0000000 -.0443567	.0006996 -.0367005
m_{θ_1}		.0236847	.0168388

*Load suspended from c.g. by sling. (All other conditions have rigidly attached load.)

5.3.4 Longitudinal Equations of Motion and Dynamic Stability Analysis

The longitudinal equations of motion used in this study are given below.

$$\left(\frac{s}{\Omega_o} + x_\mu\right)\Delta\mu + (x_\delta)\Delta\delta + \left(\frac{-s^2}{\Omega_o^2}\frac{h}{R} + \frac{s}{\Omega_o}x_{\hat{\alpha}_1} + x_{\alpha_1}\right)\Delta\alpha_1 + \left(\frac{s}{\Omega_o}x_{\hat{\beta}_1} + x_{\beta_1}\right)\Delta\beta_1 + (x_{\theta_1})\Delta\theta_1 = 0 \qquad (12)$$

$$(z_\mu)\Delta\mu + \left(\frac{s}{\Omega_o} + z_\delta\right)\Delta\delta + (z_{\alpha_1})\Delta\alpha_1 + \left(\frac{s}{\Omega_o}z_{\hat{\beta}_1} + z_{\beta_1}\right)\Delta\beta_1 + (z_{\theta_1})\Delta\theta_1 = 0 \qquad (13)$$

$$(m_\mu)\Delta\mu + (m_\delta)\Delta\delta \left(\frac{s^2}{\Omega_o^2} + \frac{s}{\Omega_o}m_{\hat{\alpha}_1} + m_{\alpha_1}\right)\Delta\alpha_1 + \left(\frac{s}{\Omega_o}m_{\hat{\beta}_1} + m_{\beta_1}\right)\Delta\beta_1 + (m_{\theta_1})\Delta\theta_1 = 0 \qquad (14)$$

$$(\beta_{1_\mu})\Delta\mu + (\beta_{1_\delta})\Delta\delta + (\beta_{1_{\alpha_1}})\Delta\alpha_1 + \left(\frac{s}{\Omega_o}\beta_{1_{\hat{\beta}_1}} - 1\right)\Delta\beta_1 + (\beta_{1_{\theta_1}})\Delta\theta_1 = 0 \qquad (15)$$

These equations are derived in Reference 4 and are identical to equations (A.46), (A.47), (A.48), and (A.49) of that report.

Rewriting Equations (12) through (15) in matrix form, we have:

$$\begin{bmatrix} \left(\frac{s}{\Omega_o} + x_\mu\right) & (x_\delta) & \left(\frac{-s^2}{\Omega_o^2}\frac{h}{R} + \frac{s}{\Omega_o}x_{\hat{\alpha}_1} + x_{\alpha_1}\right) & \left(\frac{s}{\Omega_o}x_{\hat{\beta}_1} + x_{\beta_1}\right) \\ (z_\mu) & \left(\frac{s}{\Omega_o} + z_\delta\right) & (z_{\alpha_1}) & \left(\frac{s}{\Omega_o}z_{\hat{\beta}_1} + z_{\beta_1}\right) \\ (m_\mu) & (m_\delta) & \left(\frac{s^2}{\Omega_o^2} + \frac{s}{\Omega_o}m_{\hat{\alpha}_1} + m_{\alpha_1}\right) & \left(\frac{s}{\Omega_o}m_{\hat{\beta}_1} + m_{\beta_1}\right) \\ (\beta_{1_\mu}) & (\beta_{1_\delta}) & (\beta_{1_{\alpha_1}}) & \left(\frac{s}{\Omega_o}\beta_{1_{\hat{\beta}_1}} - 1\right) \end{bmatrix} \begin{Bmatrix} \Delta\mu \\ \Delta\delta \\ \Delta\alpha_1 \\ \Delta\beta_1 \end{Bmatrix} = \begin{Bmatrix} -x_{\theta_1} \\ -z_{\theta_1} \\ -m_{\theta_1} \\ -\beta_{1_{\theta_1}} \end{Bmatrix} \Delta\theta_1$$

The matrix form of the equations provides the following transfer function, in determinant form, of pitch attitude response to longitudinal cyclic control input.

$$\frac{\Delta\alpha_1(s)}{\Delta\theta_1(s)} = \frac{\begin{vmatrix} \left(\frac{s}{\Omega_o} + x_\mu\right) & (x_\delta) & (-x_{\theta_1}) & \left(\frac{s}{\Omega_o} x_{\hat{\beta}_1} + x_{\beta_1}\right) \\ (z_\mu) & \left(\frac{s}{\Omega_o} + z_\delta\right) & (-z_{\theta_1}) & \left(\frac{s}{\Omega_o} z_{\hat{\beta}_1} + z_{\beta_1}\right) \\ (m_\mu) & (m_\delta) & (-m_{\theta_1}) & \left(\frac{s}{\Omega_o} m_{\hat{\beta}_1} + m_{\beta_1}\right) \\ (\beta_{1_\mu}) & (\beta_{1_\delta}) & (-\beta_{1_{\beta_1}}) & \left(\frac{s}{\Omega_o} \beta_{1_{\hat{\beta}_1}} - 1\right) \end{vmatrix}}{\begin{vmatrix} \left(\frac{s}{\Omega_o} + x_\mu\right) & (x_\delta) & \left(\frac{s^2}{\Omega_o^2}\frac{h}{R} + \frac{s}{\Omega_o} x_{\hat{\alpha}_1} + x_{\alpha_1}\right) & \left(\frac{s}{\Omega_o} x_{\hat{\beta}_1} + x_{\beta_1}\right) \\ (z_\mu) & \left(\frac{s}{\Omega_o} + z_\delta\right) & (z_{\alpha_1}) & \left(\frac{s}{\Omega_o} z_{\hat{\beta}_1} + z_{\beta_1}\right) \\ (m_\mu) & (m_\delta) & \left(\frac{s^2}{\Omega_o^2} + \frac{s}{\Omega_o} m_{\hat{\alpha}_1} + m_{\alpha_1}\right) & \left(\frac{s}{\Omega_o} m_{\hat{\beta}_1} + m_{\beta_1}\right) \\ (\beta_{1_\mu}) & (\beta_{1_\delta}) & (\beta_{1_{\alpha_1}}) & \left(\frac{s}{\Omega_o} \beta_{1_{\hat{\beta}_1}} - 1\right) \end{vmatrix}}$$

Expanding these two determinants results in the ratio of two polynomials in the Laplace operator, s.

$$\frac{\Delta\alpha_1(s)}{\Delta\theta_1(s)} = \frac{a_3 s^3 + a_2 s^2 + a_1 s + a_0}{b_5 s^5 + b_4 s^4 + b_3 s^3 + b_2 s^2 + b_1 s + b_0} \qquad (16)$$

Setting the denominator equal to zero, we have:

$$b_5 s^5 + b_4 s^4 + b_3 s^3 + b_2 s^2 + b_1 s + b_0 = 0 \qquad (17)$$

This is the characteristic equation of the longitudinal dynamics. The roots of this equation provide the stability characteristics of the longitudinal modes of motion. These roots are summarized in Table 2.

The Laplace transform of the pitch response ($\Delta\alpha(s)$) to a unit step control input ($\Delta\theta_1(s) = 1/s$) is obtained by multiplying the transfer function (16) by ($1/s$).

$$\Delta\alpha_1(s) = \frac{a_3s^3 + a_2s^2 + a_1s + a_0}{s(b_5s^5 + b_4s^4 + b_3s^3 + b_2s^2 + b_1s + b_0)} \qquad (18)$$

The time response ($\Delta\alpha_1(t)$) to a unit step control input is obtained by finding the inverse Laplace transform of Equation (18). Therefore:

$$\Delta\alpha_1(t) = \mathcal{L}^{-1} \frac{a_3s^3 + a_2s^2 + a_1s + a_0}{s(b_5s^5 + b_4s^4 + b_3s^3 + b_2s^2 + b_1s + b_0)}$$

(*)

Derivation of Horizontal Force Due to Tip-Mounted Engine Nacelles:

The airloads on the tip-mounted nacelles produce a net horizontal force aft. This net force will be derived in terms of the drag and lift forces on the nacelle in the horizontal plane. Figure 17 illustrates the components of forces and velocity in the horizontal plane.

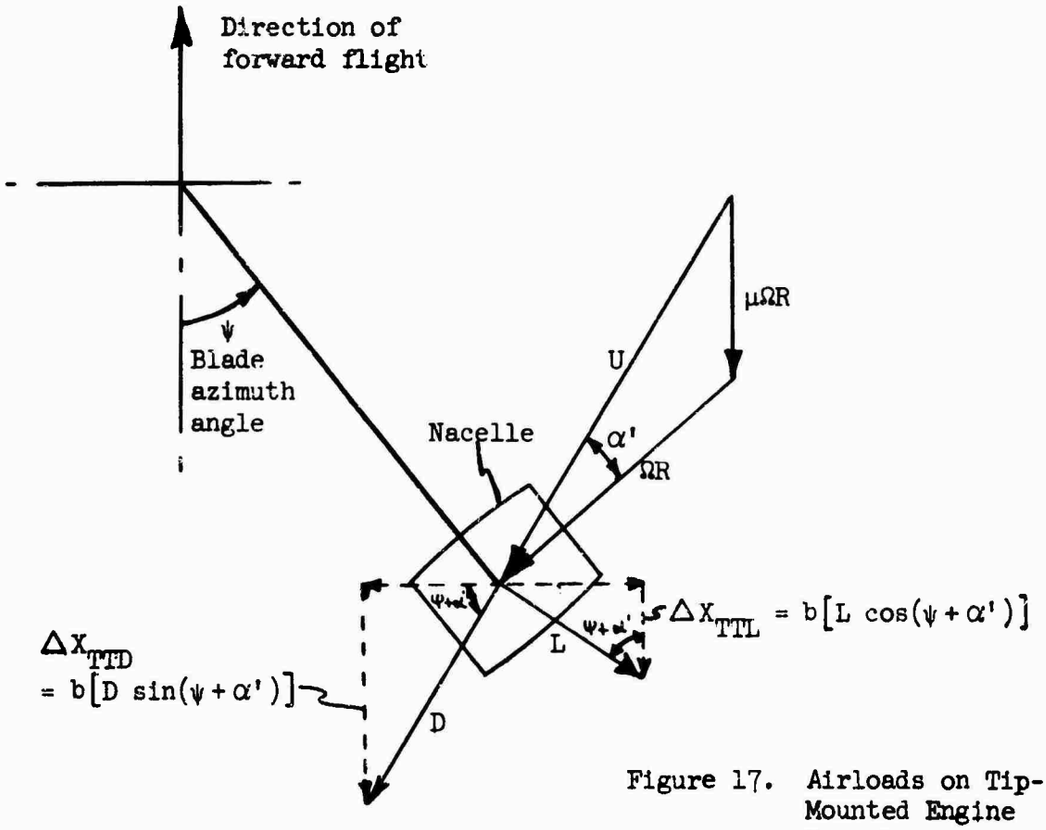

Figure 17. Airloads on Tip-Mounted Engine Nacelles.

*This procedure was carried out to calculate the time responses summarized in Table 1.

U = total velocity relative to the nacelle from Figure 17

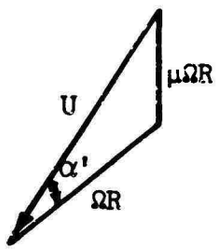

or,

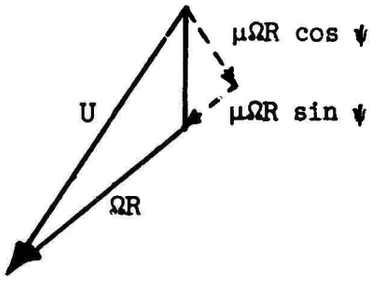

$$U^2 = (\Omega R + \mu\Omega R \sin\psi)^2 + (\mu\Omega R \cos\psi)^2$$
$$= (\Omega R)^2(1 + \mu^2 + 2\mu \sin\psi)$$

α' = relative angle between the nacelle and the total relative velocity.

$$\tan\alpha' = \frac{\mu \cos\psi}{1 + \mu \sin\psi} = \alpha', \text{ assuming } \alpha' \text{ small}$$

The contribution of the tip-mounted engine nacelles will be calculated in two parts:

(1) ΔX_{TTD} = horizontal rotor force due to nacelle drag

(2) ΔX_{TTL} = horizontal rotor force due to nacelle lift

Calculation of ΔX_{TTD}: From Figure 17 we see that at any given ψ,

$$\Delta X_{TTD} = b\left[D \sin(\psi + \alpha')\right]$$

where: b = number of rotor blades.

The sine of the sum of two angles may be written:

$$\sin(\psi + \alpha') = \sin\psi \cos\alpha' + \cos\psi \sin\alpha'$$

Substituting: $\Delta X_{TTD} = bD(\sin\psi \cos\alpha' + \cos\psi \sin\alpha')$

For α' a small angle,

$$\Delta X_{TTD} \sim bD(\sin\psi + \alpha' \cos\psi)$$

the average ΔX_{TTD} for a full rotor rotation is given by:

$$\Delta X_{TTD} = \frac{1}{2\pi}\int_0^{2\pi} \Delta X_{TTD} d\psi = \frac{b}{2\pi}\int_0^{2\pi} D(\sin\psi + \alpha' \cos\psi)d\psi$$

where: $D = \frac{1}{2}\rho U^2 C_{D_{TT}} S_{TT} = \frac{1}{2}\rho(\Omega R)^2(1 + \mu^2 + 2\mu \sin\psi)C_{D_{TT}} S_T$

Substituting:

$$\Delta X_{TTD_{avg.}} = \frac{b}{2\pi}\int_0^{2\pi} \frac{\rho}{2}(\Omega R)^2 C_{D_{TT}} S_{TT}(1+\mu^2+2\mu \sin\psi)(\sin\psi + \alpha'\cos\psi)d\psi$$

Expanding:

$$\Delta X_{TTD_{avg.}} = \frac{b}{4\pi}\rho(\Omega R)^2 C_{D_{TT}} S_{TT}\int_0^{2\pi}(\sin\psi + \mu^2\sin\psi + 2\mu\sin^2\psi)d\psi$$

$$+ \frac{b}{4\pi}\rho(\Omega R)^2 C_{D_{TT}} S_{TT}\int_0^{2\pi}\alpha'(\cos\psi + \mu^2\cos\psi + 2\mu\sin\psi\cos\psi)d\psi$$

Assume α' may be considered as a constant in the second integral. The validity of this assumption is based on the fact that α' will oscillate between finite, limited values, and the average value may be assumed in the integral. With this assumption the above integral reduces to:

$$\Delta X_{TTD_{avg.}} = \frac{b}{4\pi}\rho(\Omega R)^2 C_{D_{TT}} S_{TT}(2\mu\pi)$$

Finally:

$$\Delta X_{TTD_{avg.}} = \frac{b}{2}\rho(\Omega R)^2 C_{D_{TT}} S_{TT}\mu$$

Calculation of ΔX_{TTL}:

From Figure 17, for any given ψ:

$$\Delta X_{TTL} = b\left[L\cos(\psi + \alpha')\right]$$

The average ΔX_{TTL} for a full rotor rotation is given by:

$$\Delta X_{TTL_{avg.}} = \frac{1}{2\pi}\int_0^{2\pi}\Delta X_{TTL}d\psi = \frac{b}{2\pi}\int_0^{2\pi} L\cos(\psi+\alpha')d\psi$$

where: $L = \frac{1}{2}\rho U^2\left(\frac{\partial C_L}{\partial\alpha}\right)\alpha' S_{TT}$

$$= \frac{1}{2}\rho(\Omega R)^2(1+\mu^2+2\mu\sin\psi)\left(\frac{\partial C_L}{\partial\alpha}\right)\alpha' S_{TT}$$

$$\alpha' = \frac{\mu\cos\psi}{1+\mu\sin\psi}\text{, for small angles}$$

Substituting for L and α':

$$\Delta X_{TTL_{avg.}} = \frac{b}{2}\rho(\Omega R)^2\left(\frac{\partial C_L}{\partial\alpha}\right)S_{TT}\frac{1}{2\pi}\int_0^{2\pi}\xi d\psi$$

where:

$$\frac{1}{2\pi}\int_0^{2\pi} \xi\, d\psi = \frac{1}{2\pi}\int_0^{2\pi} (1+\mu^2+2\mu\sin\psi)\left(\frac{\mu\cos\psi}{1+\mu\sin\psi}\right)\cos\left[\psi+\left(\frac{\mu\cos\psi}{1+\mu\sin\psi}\right)\right] d\psi$$

This definite integral was evaluated for some specific values of μ, with the result:

$$\frac{1}{2\pi}\int_0^{2\pi} \xi\, d\psi = \begin{cases} 0\ , & \mu = 0 \\ .0785, & \mu = .155 \\ .1340, & \mu = .26 \end{cases}$$

This is very nearly a linear relationship, leading to the approximation

$$\frac{1}{2\pi}\int_0^{2\pi} \xi\, d\psi \sim (.51)\mu$$

Finally, substituting for $\frac{1}{2\pi}\int_0^{2\pi} \xi\, d\psi$:

$$\Delta X_{TTL_{avg.}} = \frac{b}{2}\rho(\Omega R)^2\left(\frac{\partial C_L}{\partial\alpha}\right) S_{TT}(.51)\mu$$

The combined effect of the tip-mounted engine nacelle drag and lift on the horizontal rotor force, ΔX_{TT}, may now be summarized:

$$\Delta X_{TT} = \Delta X_{TTD_{avg.}} + \Delta X_{TTL_{avg.}}$$

$$\Delta X_{TT} = \frac{b}{2}\rho(\Omega R)^2 C_{D_{TT}} S_{TT}\mu + \frac{b}{2}\rho(\Omega R)^2\left(\frac{\partial C_L}{\partial\alpha}\right) S_{TT}(.51)\mu$$

This reduces to the final equation,

$$\Delta X_{TT} = \frac{b}{2}\rho(\Omega R)^2 S_{TT}\mu\left[C_{D_{TT}} + .51\left(\frac{\partial C_L}{\partial\alpha}\right)_{TT}\right] \qquad (19)$$

where: b = number of blades

S_{TT} = engine inlet area

$C_{D_{TT}}$ = nacelle drag coefficient, based on S_{TT}

$\left(\frac{\partial C_L}{\partial\alpha}\right)_{TT}$ = nacelle lift curve slope, based on S_{TT}

μ = advance ratio

Derivation of Moment Due to Spring Restraint:

Consider a blade in the x-y plane, at azimuth ψ.

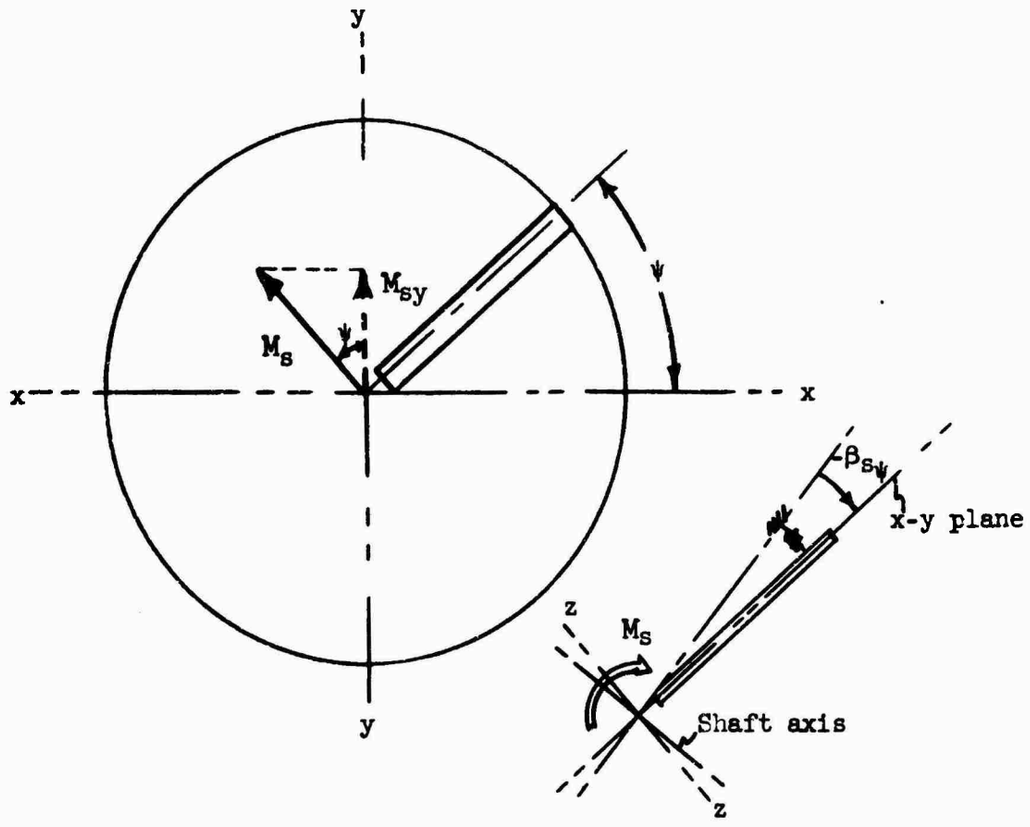

Figure 18. Spring Restraint Moment Diagram.

M_s = fuselage moment due to spring restraint, due to a single blade at azimuth ψ

$= k_\beta(-\beta_{s\psi})$

where: k_β = spring restraint per blade, ft-lb/rad.

$\beta_{s\psi}$ = blade flapping at azimuth ψ, relative to shaft

$= \beta_o + \beta_{1s} \cos \psi + \beta_{2s} \sin \psi$

M_{s_y} = pitching component of fuselage moment due to spring restraint for a single blade at azimuth ψ

$= M_s \cos \psi$

The average pitching moment for a blade, M_{s_y}, is given by:

$$M_{s_y} = b \frac{1}{2\pi} \int_0^{2\pi} \mathcal{M}_{s_y} d\psi$$

But
$$\mathcal{M}_{s_y} = \mathcal{M}_s \cos\psi = k_\beta(-\beta_{s_\psi}) \cos\psi$$
$$= -k_\beta(\beta_o + \beta_{1_s} \cos\psi + \beta_{2_s} \sin\psi) \cos\psi$$

$$M_{s_y} = \frac{-bk_\beta}{2\pi} \int_0^{2\pi} (\beta_o \cos\psi + \beta_{1_s} \cos^2\psi + \beta_{2_s} \sin\psi \cos\psi) d\psi$$
$$= \frac{-bk_\beta}{2\pi} (\beta_{1_s}\pi)$$
$$M_{s_y} = \frac{bk_\beta(-\beta_{1_s})}{2} \qquad (20)$$

The equations of Reference 4 are derived to include the effects of an offset hinge. It is desired to treat the spring restraint as an equivalent offset hinge to facilitate analysis.

The pitching moment due to offset hinges, M_y, is given by:

$$M_y = \frac{bm_b ed\Omega^2}{2} (-\beta_{1_s}) \qquad \text{(eq. A.31, Reference 4)}$$

Equating the pitching moments due to offset hinges and spring restraint,

$$M_y = M_{s_y}$$
$$\frac{bm_b ed\Omega^2}{2} (-\beta_{1_s}) = \frac{bk_\beta(-\beta_{1_s})}{2}$$
$$\text{"e"} = \frac{k_\beta}{m_b d\Omega^2} \quad \text{, equivalent hinge offset} \qquad (21)$$

where:

m_b = mass per blade

d = distance of blade c.g. outboard of flapping hinge

5.3.5 Analog Computer Circuit

Transient response characteristics were obtained on the PACE TR-48 analog computer. This is a fully transistorized computer, with an operating range of ±10 volts. The analog provided a simultaneous solution of the longitudinal equations of motion, Equations (12) through (15), listed on page 46. The analog circuit diagrams are shown on Figures 19 through 22, and the potentiometer settings are given in Table 13.

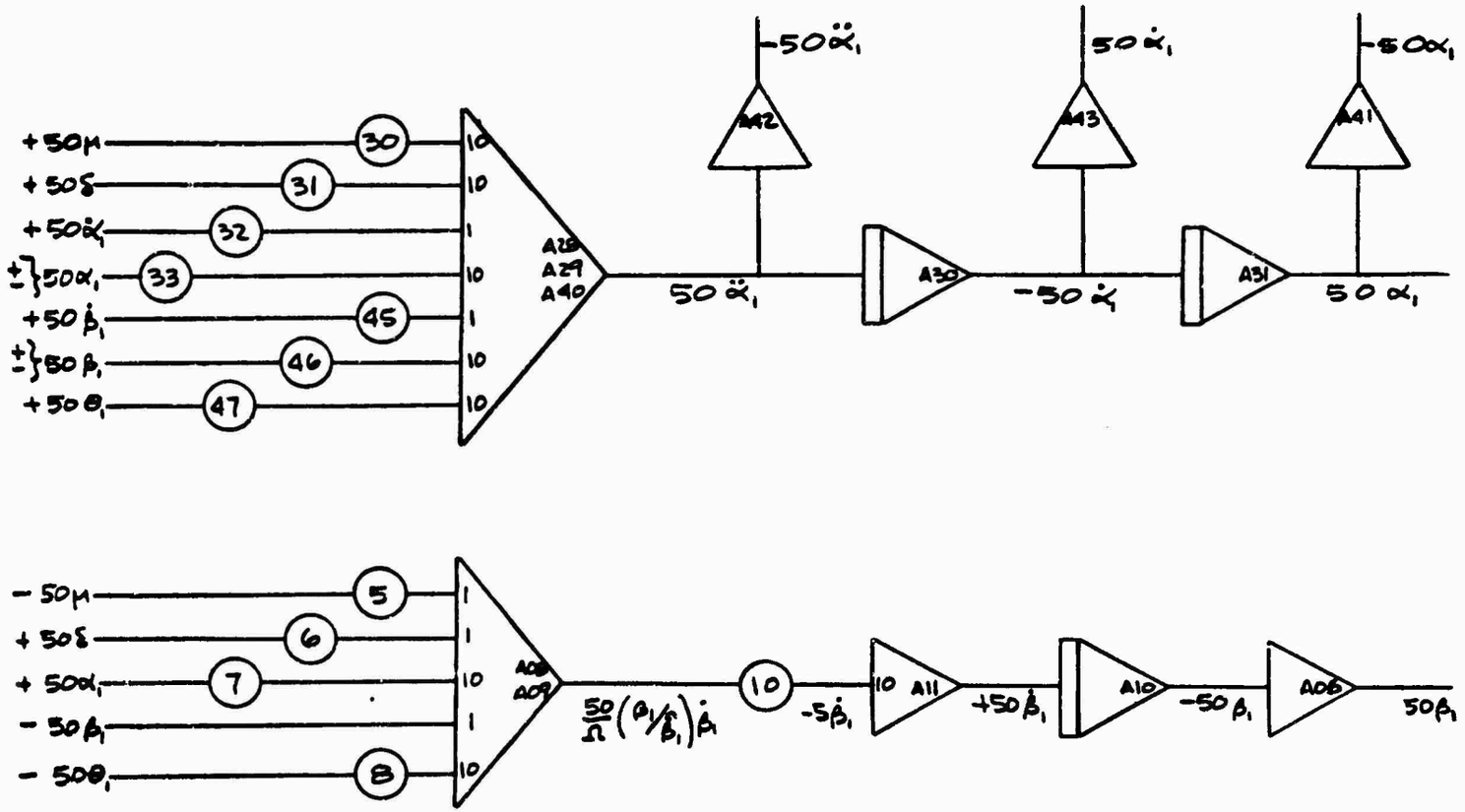

Figure 19. Analog Computer Circuits for Roter Shaft Tilt (α_1) and Tip Path Plane Tilt (β_1).

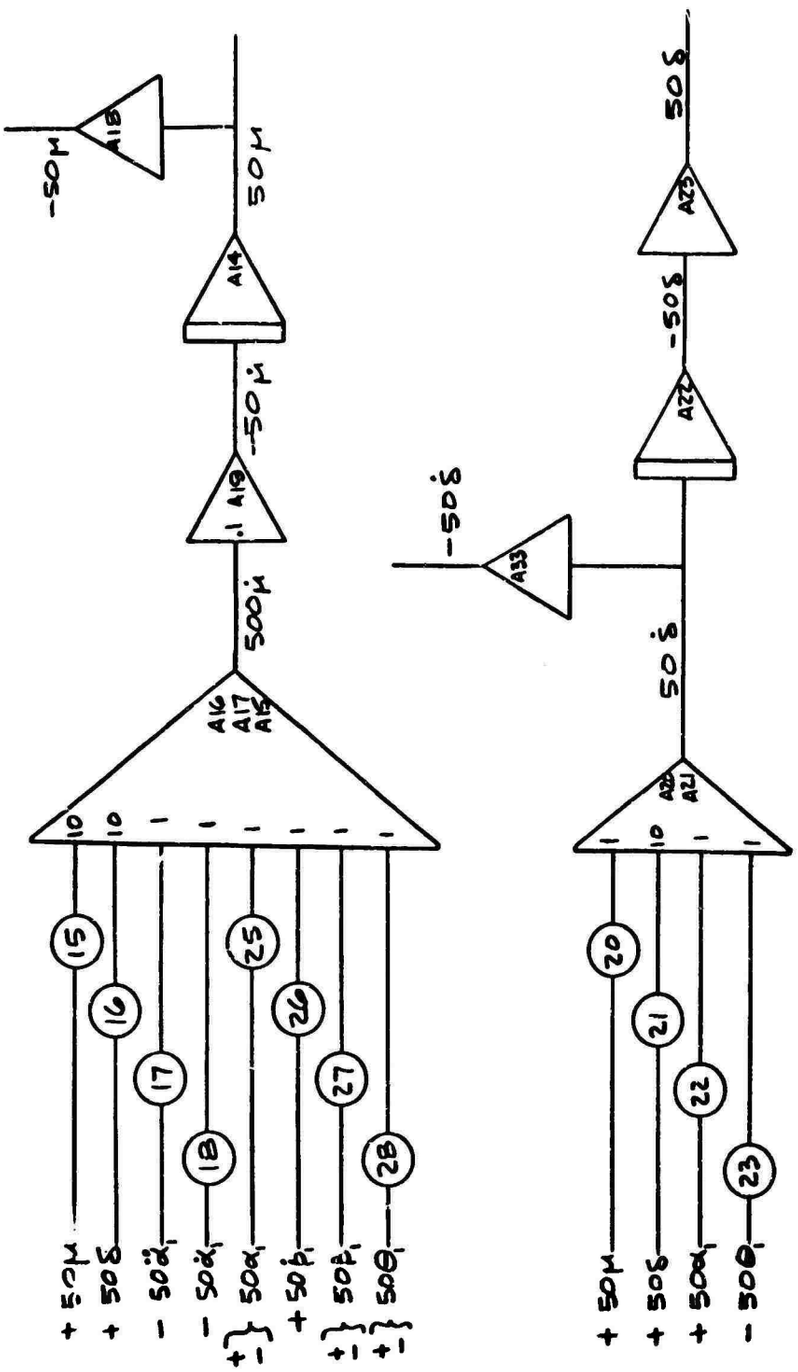

Figure 20. Analog Computer Circuits for Rotor Advance Ratio (μ) and Rotor Vertical Advance Ratio (δ).

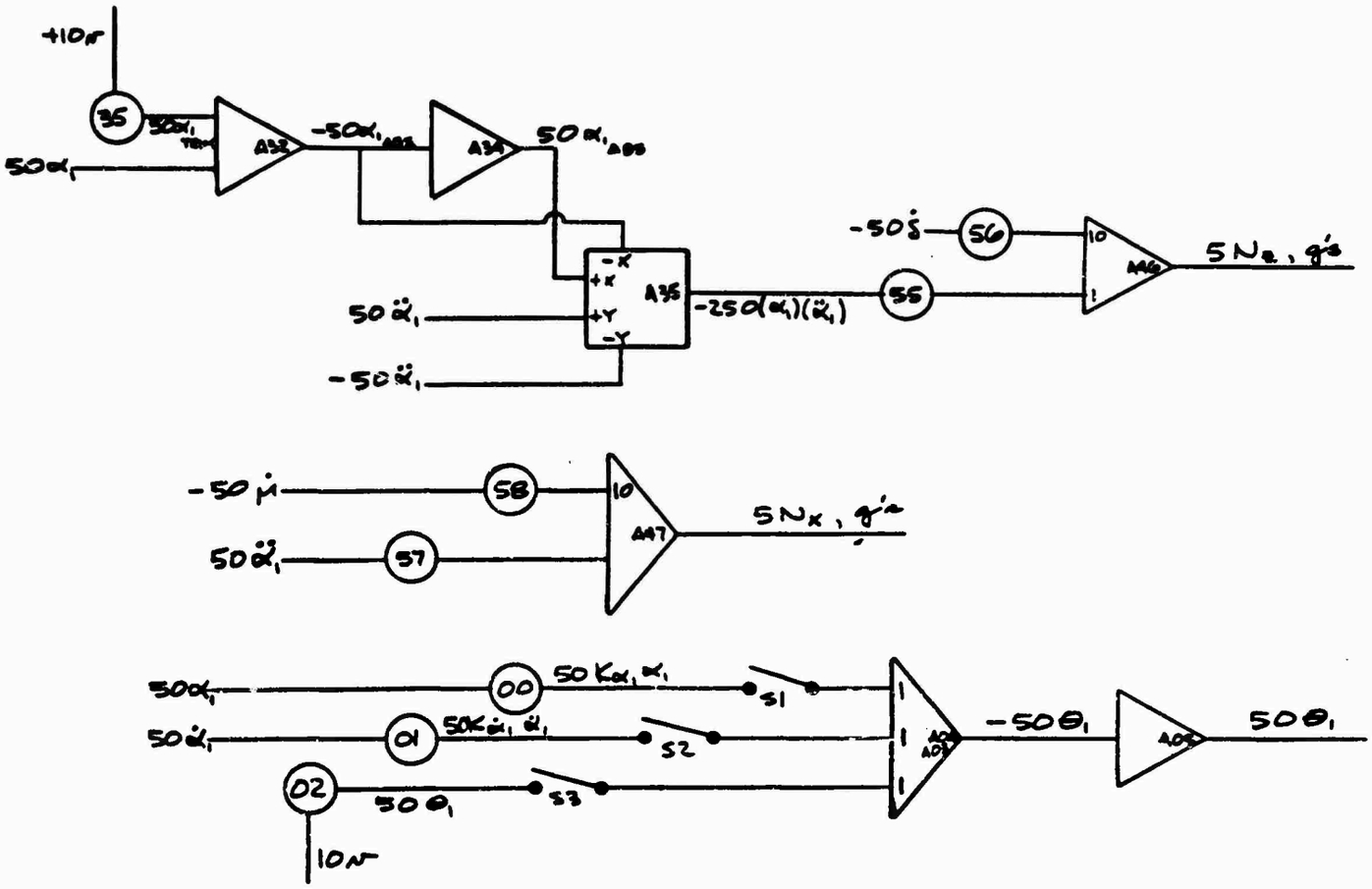

Figure 21. Analog Computer Circuits for Normal Acceleration (n_z) and Cyclic Pitch (θ_1).

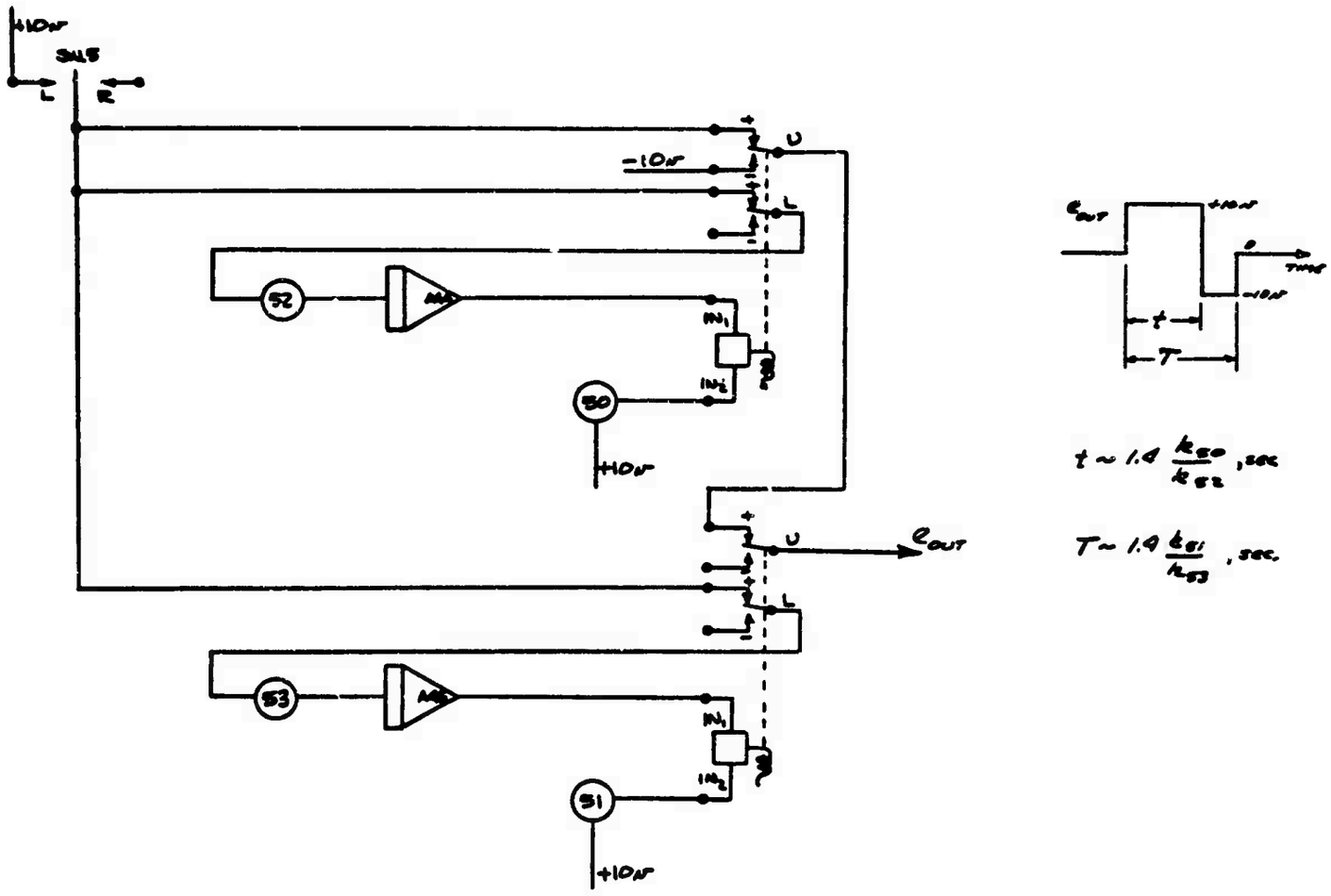

Figure 22. Analog Computer Circuit for Pilot-Applied Cyclic Pitch Input.

TABLE 13
ANALOG COMPUTER POTENTIOMETER SETTINGS

Potentiometer	Setting	Potentiometer	Setting
00	K_{α_1}	25	$\Omega x_{\alpha_1}(10)$
1	$K^{\blacklozenge}_{\alpha_1}$	26	$x^{\blacklozenge}_{\beta_1}(10)$
2	$5\theta_{1_{pilot}}$	27	$\Omega x_{\beta_1}(10)$
5	β_{1_μ}	28	$\Omega x_{\theta_1}(10)$
6	β_{1_δ}	30	$\Omega^2 m_\mu\left(\frac{1}{10}\right)$
7	$\beta_{1_{\alpha_1}}\left(\frac{1}{10}\right)$	31	$\Omega^2 m_\delta\left(\frac{1}{10}\right)$
8	$\beta_{1_{\theta_1}}\left(\frac{1}{10}\right)$	32	$\Omega m^{\blacklozenge}_{\alpha_1}$
10	$\left(\frac{\Omega}{\beta_1 \beta^{\blacklozenge}_1}\right)\left(\frac{1}{10}\right)$	33	$\Omega^2 m_{\alpha_1}\left(\frac{1}{10}\right)$
15	Ωx_μ	35	$5\alpha_{1_{trim}}$
16	Ωx_δ	45	$\Omega m^{\blacklozenge}_{\beta_1}$
17	$\frac{1}{\Omega}\frac{h}{R}$ (10)	46	$\Omega^2 m_{\beta_1}\left(\frac{1}{10}\right)$
18	$x^{\blacklozenge}_{\alpha_1}$ (10)	47	$\Omega^2 m_{\theta_1}\left(\frac{1}{10}\right)$
20	Ωz_μ	55	$\frac{h}{g}\left(\frac{1}{50}\right)$
21	$\Omega z_\delta\left(\frac{1}{10}\right)$	56	$\frac{\Omega R}{g}\left(\frac{1}{100}\right)$
22	Ωz_{α_1}	57	$\frac{h}{g}\left(\frac{1}{10}\right)$
23	Ωz_{θ_1}	58	$\frac{\Omega R}{g}\left(\frac{1}{100}\right)$

5.4 Lateral-Directional Analysis Methods

5.4.1 Lateral-Directional Equations of Motion

The lateral-directional analysis is based on the following equations of motion. These equations, plus their stability derivatives, are derived in Reference 7.

Σ side force = 0

$$(ms - Y_v)v - (mw_o s + mg\cos\theta_o + Y_\phi s)\phi + (mu_c - Y_{\dot\psi})\dot\psi = Y_{\theta_2}\theta_2 + Y_{\theta_{tr}}\theta_{tr} \tag{22}$$

Σ rolling moment = 0

$$(-\ell_v)v + (I_{\bar x\bar x}s^2 - \ell_\phi s)\phi - (I_{\bar x\bar z}s + \ell_{\dot\psi})\dot\psi = \ell_{\theta_2}\theta_2 + \ell_{\theta_{tr}}\theta_{tr} \tag{23}$$

Σ yawing moment = 0

$$(-N_v)v - (I_{\bar x\bar z}s^2 + N_\phi s)\phi + (I_{\bar z\bar z}s - N_{\dot\psi})\dot\psi = N_{\theta_2}\theta_2 + N_{\theta_{tr}}\theta_{tr} \tag{24}$$

Formulas for computing the stability derivatives appearing in Equations (22), (23), and (24) are given below:

$$Y_v = -m\Omega_o x_\mu + \left(\frac{\partial T}{\partial v}\right)_{tr} + \frac{1}{2} C_{Y_\beta}\rho V'\pi R^2 \tag{25}$$

$$Y_{\dot\psi} = m\Omega_o x_\mu \bar x - \left(\frac{\partial T}{\partial v}\right)_{tr}\bar x_{tr} + \frac{1}{2}\rho V'(a\bar x S)_{vt} \tag{26}$$

$$Y_\phi = -m\Omega_o x_\mu \bar z + m\Omega_o^2 R\, x_{\beta_1}\left(\frac{16}{\gamma\Omega}\right) + \left(\frac{\partial T}{\partial v}\right)_{tr}\bar z_{tr} \tag{27}$$

$$\ell_v = -m\Omega_o x_\mu \bar z + \left(\frac{\partial T}{\partial v}\right)_{tr}\bar z_{tr} + C_{\ell_\beta}\rho V'\pi R^3 \tag{28}$$

$$\ell_{\dot\psi} = m\Omega_o x_\mu \bar z\bar x - \left(\frac{\partial T}{\partial v}\right)_{tr}\bar z_{tr}\bar x_{tr} + \frac{1}{2}\rho V'(a\bar x\bar z S)_{vt} \tag{29}$$

$$\ell_\phi = -m\Omega_o x_\mu \bar z^2 + m\Omega_o^2 R\, x_{\beta_1}\left(\frac{16}{\gamma\Omega}\right)\bar z + \left(\frac{\partial T}{\partial v}\right)_{tr}\bar z_{tr}^2 + *\left[\frac{-bk_\beta}{2}\left(\frac{16}{\gamma\Omega}\right)\right] \tag{30}$$

$$N_v = m\Omega_o x_\mu \bar x - \left(\frac{\partial T}{\partial v}\right)_{tr}\bar x_{tr} + C_{N_\beta}\rho V'\pi R^3 \tag{31}$$

$$N_{\dot\psi} = -m\Omega_o x_\mu \bar x^2 + \left(\frac{\partial T}{\partial v}\right)_{tr}\bar x_{tr}^2 - \frac{1}{2}\rho V'(a\bar x^2 S)_{vt} \tag{32}$$

$$N_\phi = m\Omega_o x_\mu \bar x\bar z - m\Omega_o^2 R\, x_{\beta_1}\left(\frac{16}{\gamma\Omega}\right)\bar x - \left(\frac{\partial T}{\partial v}\right)_{tr}\bar x_{tr}\bar z_{tr} \tag{33}$$

*This term accounts for the main rotor spring restraint and is not included in the Reference 7 equations. It may be derived as follows:

$$(\Delta \ell_\phi)_{spring} = \frac{\partial \ell}{\partial \beta_{2_s}} \left(\frac{\Delta \beta_{2_s}}{\phi} \right)$$

$$\ell = \frac{bk_\beta(-\beta_{2_s})}{2} \quad \text{, from eq. (20)}$$

Hence:
$$\frac{\partial \ell}{\partial \beta_{2_s}} = \frac{-bk_\beta}{2}$$

Also:
$$\frac{\Delta \beta_{2_s}}{\phi} = \frac{16}{\gamma \Omega}$$

Substituting:

$$(\Delta \ell_\phi)_{spring} = \frac{-bk_\beta}{2} \left(\frac{16}{\gamma \Omega} \right)$$

Fuselage Aerodynamic Terms:

For this preliminary analysis, with the fuselage contour yet undefined, it is assumed that the body is at least neutrally stable.

$$C_{Y_\beta} = C_{\ell_\beta} = C_{N_\beta} = a_{vt} = 0$$

Main Rotor Aerodynamic Terms:

x_{β_1} - Use value calculated for longitudinal stability.

x_μ - Use value calculated for longitudinal stability minus $(\rho R/m) f_{\mu_o}$, to separate rotor term from longitudinal x_μ which includes rotor plus body effects.

Tail Rotor Term:

$$\left(\frac{\partial T}{\partial v} \right)_{tr} = \frac{-\rho a b c_o R V_T}{4} \left[(B^2 - x_h^2) - (B^3 - x_h^3) \frac{2}{3} t \right] \qquad (34)$$

where:

a = section lift curve slope = 5.73/rad.

b = number of blades = 5

B = tip loss correction factor = .9

c_o = root chord
c_t = tip chord } = .98 ft.

R = radius = 4 ft.

$t = 1 - c_t/c_o = 0$

V_T = tip speed = 650 f.p.s.

x_n = ratio of hub to blade radius = .22

ρ = .002378 slugs/ft^3

$\left(\frac{\partial T}{\partial v}\right)_{tr}$ = -33.1 pounds/f.p.s. per rotor

This tail rotor effectiveness does not include the second order effect of the loss in effectiveness due to rotor inflow change with thrust change. This formula is felt to provide accuracy in line with the estimated values of fuselage inertias.

Stick-Fixed Dynamics:

The coefficients of the equations of motion are arranged to form the elements of the following determinant:

$$\Delta = \begin{vmatrix} (ms - Y_v) & -(mw_o s + mg \cos\theta_o + Y_{\dot{\phi}} s) & (m u_o - Y_{\dot{\psi}}) \\ (-\ell_v) & (I_{xx} s^2 - \ell_{\dot{\phi}} s) & -(I_{xz} s + \ell_{\dot{\psi}}) \\ (-N_v) & -(I_{xz} s^2 + N_{\dot{\phi}} s) & (I_{zz} s - N_{\dot{\psi}}) \end{vmatrix}$$

Expanding this determinant and setting the result equal to zero gives a fourth order equation of the form:

$$As^4 + Bs^3 + Cs^2 + Ds + E = 0$$

The roots of this equation are solved to determine the stability characteristics. These roots are summarized in Table 5.

The lateral-directional equations of motion do not have the degree of freedom in rotor flapping included in the longitudinal equations. In hover, the longitudinal equations of motion may be used to represent the lateral motion. This is easily accomplished by multiplying all the moment terms by the ratio of pitch to roll inertia. This procedure was carried out to calculate the long period hover modes listed in Table 5. This method was felt to give the best representation of these modes.

5.4.2 Roll Response at Hover

The roll response at hover was calculated with the longitudinal equations of motion. The longitudinal stability derivatives were multiplied by the ratio of pitch to roll inertias. The transfer function techniques, outlined in Section 5.3.4, was used to obtain the roll angle response to lateral cyclic output.

5.4.3 Tail Rotor Selection

The tail rotor must be sized to provide yaw rate damping and control power for maneuvering. The damping requirement was more critical than control power for this configuration.

The tail rotor contribution to yaw rate damping is given by:

$$\frac{\partial N}{\partial \dot{\psi}} = \left(\frac{\partial T}{\partial v}\right)_{tr} \bar{x}_{tr}^2 \quad , \text{ ft-lb/rad. per sec.}$$

where:

$$\left(\frac{\partial T}{\partial v}\right)_{tr} = \frac{-\rho a b c_o R V_T}{4}\left[(B^2 - x_h^2) - (B^3 - x_h^3)\frac{2}{3}t\right] \qquad (34)$$

The tail rotor radius, R, is limited by clearance from the main rotor and ground vehicles to 4 feet. Other parameters were selected or determined to be the following:

$$\rho = .002378 \text{ slugs/ft}^3$$
$$a = 5.73/\text{rad.}$$
$$V_T = 650 \text{ f.p.s.}$$
$$B = .9$$
$$x_h = .22$$
$$C_T = 0$$

The damping may now be expressed as:

$$\frac{\partial N}{\partial \dot{\psi}} = -6.75\, b c_o\, \bar{x}_{tr}^2$$

or:

$$(bc_o)_{req'd} = -\left(\frac{1}{6.75}\right)\left(\frac{1}{\bar{x}_{tr}}\right)^2 \left(\frac{\partial N}{\partial \dot{\psi}}\right)_{req'd}$$

From Paragraph 3.3.19, Reference 1:

$$\left(\frac{\partial N}{\partial \dot{\psi}}\right)_{req'd} = -27(I_z)^{.7} \quad , \text{ ft-lb/rad. per sec.}$$

The tail rotor blade requirements are calculated and summarized in Table 14.

TABLE 14
TAIL ROTOR BLADE REQUIREMENTS

Gross Weight	c.g.	$\bar{x}_{tr}$	I_z	$(\partial N/\partial \dot{\psi})_{reqd} = -27(I_z)^{.7}$	$(bc_o)_{reqd} = -\frac{1}{6.75}\left(\frac{1}{x_{tr}}\right)^2\left(\frac{\partial N}{\partial \dot{\psi}}\right)_{reqd}$
lb.		ft.	slug-ft^2	$\frac{\text{ft-lb.}}{\text{rad/sec.}}$	ft.
39,200	mid	37.9	81,400	-74,100	7.64
71,700	mid	38.0	117,500	-95,500	9.80
71,700	aft	37.5	78,900	-72,400	7.63

The maximum value of $(bc_o)_{reqd}$ is 9.8 from Table 14. Plotting this product for single and dual tail rotors, we have:

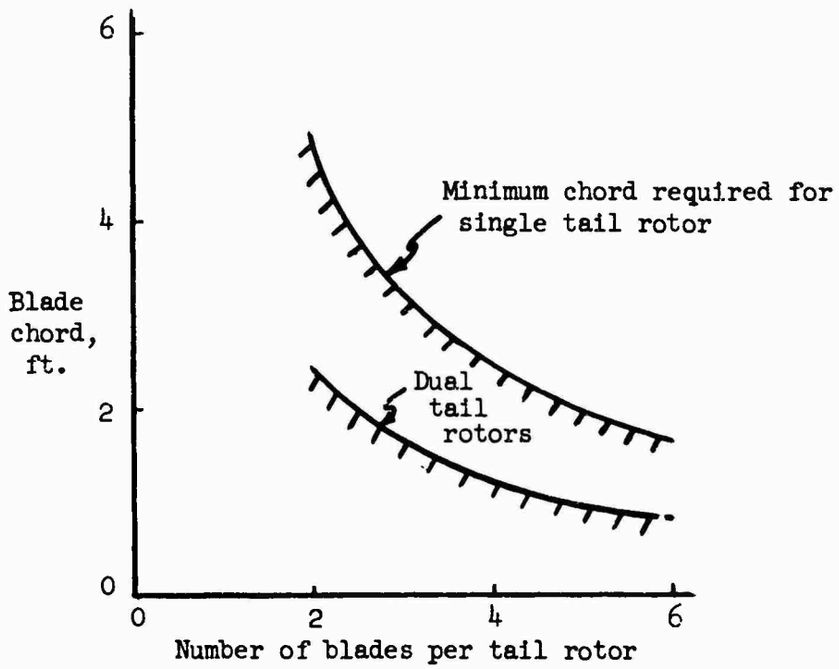

Figure 23. Tail Rotor Selection Chart.

The following tail rotor configuration was selected from Figure 23:

Number of tail rotors	= 2
Number of blades per rotor	= 5
Blade chord	= .98 ft.

The single tail rotor was rejected as an impractical configuration. The dual tail rotor offers the advantage of improved location with respect to the wake of the blunt cargo package, as well as being a more realistic rotor.

The objective of this study was to show the stability and control characteristics for a realistic helicopter mated to the selected main rotor system. Sufficient time was not available to optimize the helicopter configuration. Additional study may show a single tail rotor to be preferable if it is mounted aft and above the main rotor.

5.4.4. Yaw Response at Hover

The equation of motion for yaw, Equation (24), may be simplified in hover to

$$(I_{\bar{z}\bar{z}}s - N_{\dot{\psi}})\dot{\psi} = N_{\theta_{tr}}\theta_{tr}$$

Let $N_{\theta_{tr}}\theta_{tr} = \Delta T_{tr}\bar{x}_{tr}$

where ΔT_{tr} = increment in tail rotor thrust due to rudder pedal deflection.

Substituting: $(I_{\bar{z}\bar{z}}s - N_{\dot{\psi}})\dot{\psi} = \Delta T_{tr}\bar{x}_{tr}$

Dividing thru by $I_{\bar{z}\bar{z}}$:

$$(s - \frac{N_{\dot{\psi}}}{I_{\bar{z}\bar{z}}})\dot{\psi} = \Delta T_{tr}\left(\frac{\bar{x}_{tr}}{I_{\bar{z}\bar{z}}}\right)$$

The solution to this differential equation will give the yaw response to a rudder pedal input. For the forcing function, ΔT_{tr}, applied as a step input, the solution to this differential equation is given by Equation (35). This equation was used to calculate the yaw angle responses listed in Table 4.

$$\psi = \left(\frac{N_{\dot{\psi}}}{I_{\bar{z}\bar{z}}}\right)^{-2}\left[e^{(N_{\dot{\psi}}/I_{\bar{z}\bar{z}})t} - \left(\frac{N_{\dot{\psi}}}{I_{\bar{z}\bar{z}}}\right)t - 1\right]\left(\frac{\bar{x}_{tr}}{I_{\bar{z}\bar{z}}}\right)\Delta T_{tr} \qquad (35)$$

The yaw rate damping term, $N_{\dot{\psi}}$, used in the above formula, was calculated by Equation (32). The relationship of tail rotor thrust to tail rotor collective pitch was obtained using the following set of equations:

$$\theta_{tr} = \alpha_{tr} + \tan^{-1} \frac{(u_i)_{tr} + V_{\text{side wind}}}{.75\ V_T} \tag{36}$$

where:
$$\alpha_{tr} = \frac{6T_{tr}}{C_{L\alpha} \rho V_T^2 RB^3 bc} \tag{37}$$

For hovering in still air:

$$(u_i)_{tr} = \left\{ \frac{-u_{MR}^2 + \left[u_{MR}^4 + \left(\frac{T_{tr}}{\rho \pi B^2 R^2} \right)^2 \right]^{\frac{1}{2}}}{2} \right\}^{\frac{1}{2}} \tag{38}$$

u_{MR} = main rotor downwash at the tail rotor.

For hovering in 35-knot side wind:

$$(u_i)_{tr} = \frac{-V_{\text{side wind}} + \left[V_{\text{side wind}}^2 + \frac{2T_{tr}}{\rho \pi (BR)^2} \right]^{\frac{1}{2}}}{2} \tag{39}$$

Note: u_{MR} may be ignored in the presence of a large crosswind.

Each tail rotor must be treated separately when calculating T_{tr} versus θ_{tr} in order to correlate the correct induced velocity with tail rotor collective pitch. Equations (36) through (39) were used to calculate the thrust curves of Figure 9, from which ΔT_{tr} was obtained.

5.5 Control Power and Damping Criteria for Heavy-Lift Helicopters

The control power requirements of MIL-H-8501A, Reference 1, are felt to be unrealistic for heavy weight helicopters. This military specification states control power requirements in terms of a minimum allowable displacement of helicopter attitude resulting from a step control application. The required attitude displacement is given by:

$$\left.\begin{matrix} \Delta\alpha_1 \\ \text{or} \quad \Delta\phi \end{matrix}\right\} = \frac{K}{\sqrt[3]{W_G + 1000}} \quad \text{, degrees}$$

where K depends on the magnitude of control input and the axis of interest. This formula has provided an adequate criteria as a function of gross weight for nominal weight helicopters, but is not adequate for very heavy gross weights.

The angular acceleration due to a given control input is considered to be a more basic criteria. Since the angular acceleration is determined by dividing the control moment by the helicopter inertia, weight effects are inherently accounted for. Preferred levels of angular acceleration and damping have been determined from helicopter flight test, and are presented in Reference 8, NASA TN D-58. This information has been used as a design objective for the Model 1108. The Reference 8 boundaries will next be substantiated by comparison with additional NASA references. The Model 1108 characteristics will then be compared with the Reference 8 boundaries and the requirements of MIL-H-8501A.

5.5.1 Comparison of Pilot Opinion Boundaries

Pilot opinion boundaries for roll and pitch handling qualities are shown in Figures 24 and 25. These boundaries were taken from three separate NASA studies, described below.

> Reference 8, NASA TN D-58: A flight test research program conducted with the S-51 helicopter. The boundaries are related to characteristics for visual and instrument flight operations.
>
> Reference 9, NASA TN D-792: A piloted simulator investigation to establish attitude control requirements for hovering flight. Boundaries are given in terms of the "Cooper Pilot Opinion Rating System."
>
> Reference 10, NASA TN D-1328: A flight test program conducted with the X-14A VTOL research vehicle to establish handling qualities requirements during hovering under visual flight conditions. Boundaries are given in terms of the "Cooper Pilot Opinion Rating System."

A direct comparison of these pilot opinion boundaries is not possible because of the differences in test vehicles and rating systems. The latter two references relate to handling qualities, generally, whereas the first reference differentiates between instrument and visual flight operations. Regardless of the cited differences existing in the three references, the latter two references do substantiate the preferred level of control power established by the first. One exception to this is the low level of control power indicated by Reference 10 for the pitch axis. No apparent reason is available for this discrepancy.

It seems reasonable to interpret the "desirable" (good handling qualities for instrument flight operations) boundary of Reference 8 as indicative of preferred characteristics for precision visual flying. This should be an optimum criteria for design, and was used as a design objective for the Model 1108.

5.5.2 Model 1108 Control Power

Model 1108 control power and damping, for several loading conditions, are shown on Figures 26 through 29. These conditions were calculated using Equations (40) through (43), developed at the end of this section. Also shown on these figures are pilot opinion boundaries of NASA TN D-58 and curves corresponding to the requirements of MIL-H-8501A. The constant weight curves, corresponding to the requirements of MIL-H-8501A, are derived as follows:

For a single degree of freedom system with rate damping and a step input forcing function, we have,

$$\delta = \frac{F}{D^2}\left[e^{(D)t} - (D)t - 1\right]$$

where: δ = angular displacement at time, t, radians.

F = magnitude of step input forcing function, rad/sec.^{2}

D = rate damping, $\frac{\text{rad/sec}^2}{\text{rad/sec.}} = \frac{1}{\text{sec.}}$

t = time from initiation of step input, seconds.

For $\delta = \frac{K}{\sqrt[3]{W_G + 1000}}$, deg., from MIL-H-8501A, we have

$$\frac{1}{57.3}\left(\frac{K}{\sqrt[3]{W_G + 1000}}\right) = \frac{F}{D^2}\left[e^{(D)t} - (D)t - 1\right]$$

This equation provides a relationship of damping versus control power, at constant gross weight, corresponding to the requirements of MIL-H-8501A.

Figures 27 and 29 show that the military specification requirement brackets the "desirable" boundary for gross weights of 2,000 to 10,000 pounds, but specifies too little control power for the heavier gross weights. The Model 1108 has been designed to provide control power approaching the "desirable" boundary, as an optimum, rather than the minimum military specification requirement.

Figures 26 through 29 show the Model 1108 to meet the control power objective, with the spring restraint system included in the design. The spring restraint also has a significant effect on the damping. Even without the spring restraint, the control power would meet the MIL-H-8501A requirement. Pitch and roll damping, while not within the desirable boundary, was shown in Sections 3.1.2.3 and 3.2.2 to exceed the MIL-H-8501A requirements. Some stability augmentation should be added to achieve preferable damping.

5.5.3 Equations for Control Power and Damping at Hover

The Model 1108 control power and damping points shown on Figures 26 through 29 were obtained from the following expressions:

Control power may be calculated by

$$\frac{d\ddot{\alpha}}{d\theta_1} = \frac{Th}{I_{\bar{y}\bar{y}}} \quad , \qquad \text{rad/sec}^2\text{/rad.} \quad \text{(without spring restraint)}$$

The addition of the spring restraint gives

$$\left(\frac{d\ddot{\alpha}_1}{d\theta_1}\right)_{spring} = \frac{1}{I_{\bar{y}\bar{y}}} \frac{\partial M_{s_y}}{\partial \beta_{1_s}} \frac{d\beta_{1_s}}{d\theta_1}$$

From Section 5.3.4 we have

$$M_{s_y} = \frac{bk_\beta}{2}(-\beta_{1_s}) \tag{20}$$

$$\frac{\partial M_{s_y}}{\partial \beta_{1_s}} = \frac{-bk_\beta}{2}$$

At hover, blade flapping follows cyclic pitch, except for a very short time lag. Hence,

$$\frac{d\,\beta_{1_s}}{d\theta_1} = -1$$

Substituting:

$$\left(\frac{d\ddot{\alpha}_1}{d\theta_1}\right)_{spring} = \frac{bk_\beta}{2I_{\bar{y}\bar{y}}}$$

Finally:

$$\frac{d\ddot{\alpha}_1}{d\theta_1} = \frac{Th}{I_{\bar{y}\bar{y}}} + \frac{bk_\beta}{2I_{\bar{y}\bar{y}}} \quad , \text{ rad/sec}^2\text{/rad.} \quad \text{(including spring restraint)} \tag{40}$$

From Equation (10) of Reference 11, we have the damping given by:

$$\frac{d\ddot{\alpha}_1}{d\dot{\alpha}_1} = \frac{-27}{\gamma\Omega}\left(1.0 - .29\,\frac{\theta}{C_T/\sigma}\right)\frac{Th}{I_{\bar{y}\bar{y}}} \quad , \text{ per second} \quad \text{(without spring restraint)}$$

The addition of the spring restraint gives:

$$\left(\frac{d\ddot{\alpha}_1}{d\dot{\alpha}_1}\right)_{spring} = \frac{1}{I_{\bar{y}\bar{y}}} \frac{\partial M_{s_y}}{\partial \beta_{1_s}} \frac{d\beta_{1_s}}{d\dot{\alpha}_1}$$

As before, $$\frac{\partial M_{s_y}}{\partial \beta_{1_s}} = - \frac{bk_\beta}{2}$$

Also: $$\frac{d\,\beta_{1_s}}{d\alpha_1} = \frac{16}{\gamma\Omega}$$

Substituting: $$\left(\frac{d\ddot{\alpha}_1}{d\alpha_1}\right)_{spring} = \frac{-bk_\beta}{2I_{\bar{y}\bar{y}}}\left(\frac{16}{\gamma\Omega}\right)$$

Finally:

$$\frac{d\ddot{\alpha}_1}{d\dot{\alpha}_1} = - \frac{27}{\gamma\Omega}\left(1.0 - .29\,\frac{\theta}{C_T/\sigma}\right)\frac{Th}{I_{\bar{y}\bar{y}}} - \frac{bk_\beta}{2I_{\bar{y}\bar{y}}}\left(\frac{16}{\gamma\Omega}\right) \text{ per second} \quad (41)$$

(including spring restraint)

The control power and damping in roll is related to the pitch characteristics by the ratio of the inertias.

Therefore: $$\frac{d\ddot{\phi}}{d\theta_2} = \frac{I_{\bar{y}\bar{y}}}{I_{\bar{x}\bar{x}}}\left(\frac{d\ddot{\alpha}_1}{d\theta_1}\right) \text{ rad/sec}^2\text{/rad.} \quad (42)$$

and $$\frac{d\ddot{\phi}}{d\dot{\phi}} = \frac{I_{\bar{y}\bar{y}}}{I_{\bar{x}\bar{x}}}\left(\frac{d\ddot{\alpha}_1}{d\dot{\alpha}_1}\right) \text{ per second} \quad (43)$$

Boundary	Descriptive Pilot Opinion	Reference
(A)	"Desirable" - "good handling qualities for instrument flight operations"	NASA TN D-58 (Ref.8) (S-51 flight test)
(B)	"Acceptable" - "acceptable for instrument flight operations"	
(C)	"Marginal" - "acceptable for visual flight operations only"	
(1)	"Satisfactory for normal operation" (Cooper Rating = 3-1/2)	NASA TN D-792 (Ref.9) (simulator test)
(2)	---Same as above---	NASA TN D-1328 (Ref.10) (X-14A flight test)

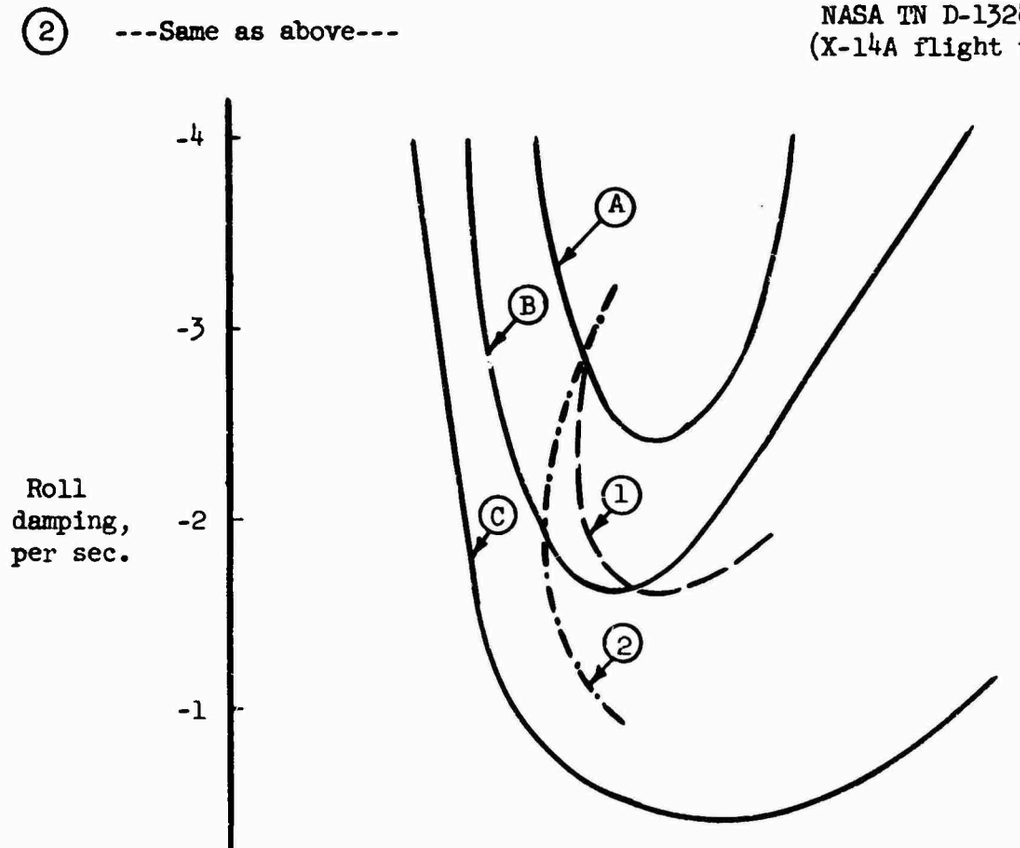

Figure 24. Pilot Opinion Comparison, Roll Axis.

Boundary	Descriptive Pilot Opinion	Reference
(A)	"Desirable" - "good handling qualities for instrument flight operations"	NASA TN D-58, (Reference 8) (S-51 flight test)
(B)	"Acceptable" - "acceptable for instrument flight operations"	
(C)	"Marginal" - "acceptable for visual flight operations only"	
(1)	"Satisfactory for normal operation" (Cooper Rating = 3-1/2)	NASA TN D-792, (Reference 9) (simulator test)
(2)	---Same as above---	NASA TN D-1328 (Reference 10) (X-14A flight test)

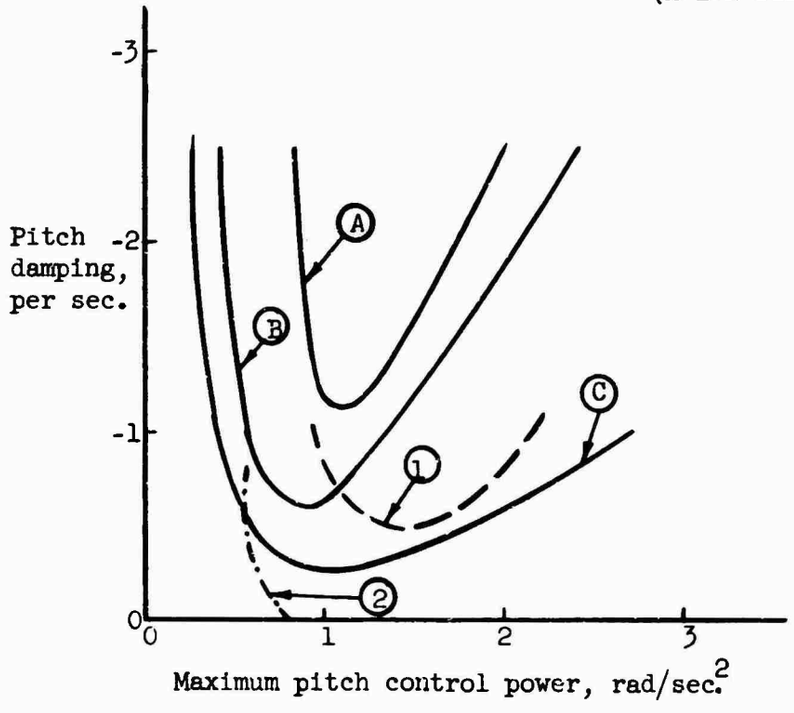

Figure 25. Pilot Opinion Comparison, Pitch Axis.

Boundary	Descriptive Pilot Opinion	Reference
(A)	"Desirable" - "good handling qualities for instrument flight operations"	NASA TN D-58 (Reference 8) (S-51 flight test)
(B)	"Acceptable" - "acceptable for instrument flight operations"	
(C)	"Marginal" - "acceptable for visual flight operations only"	

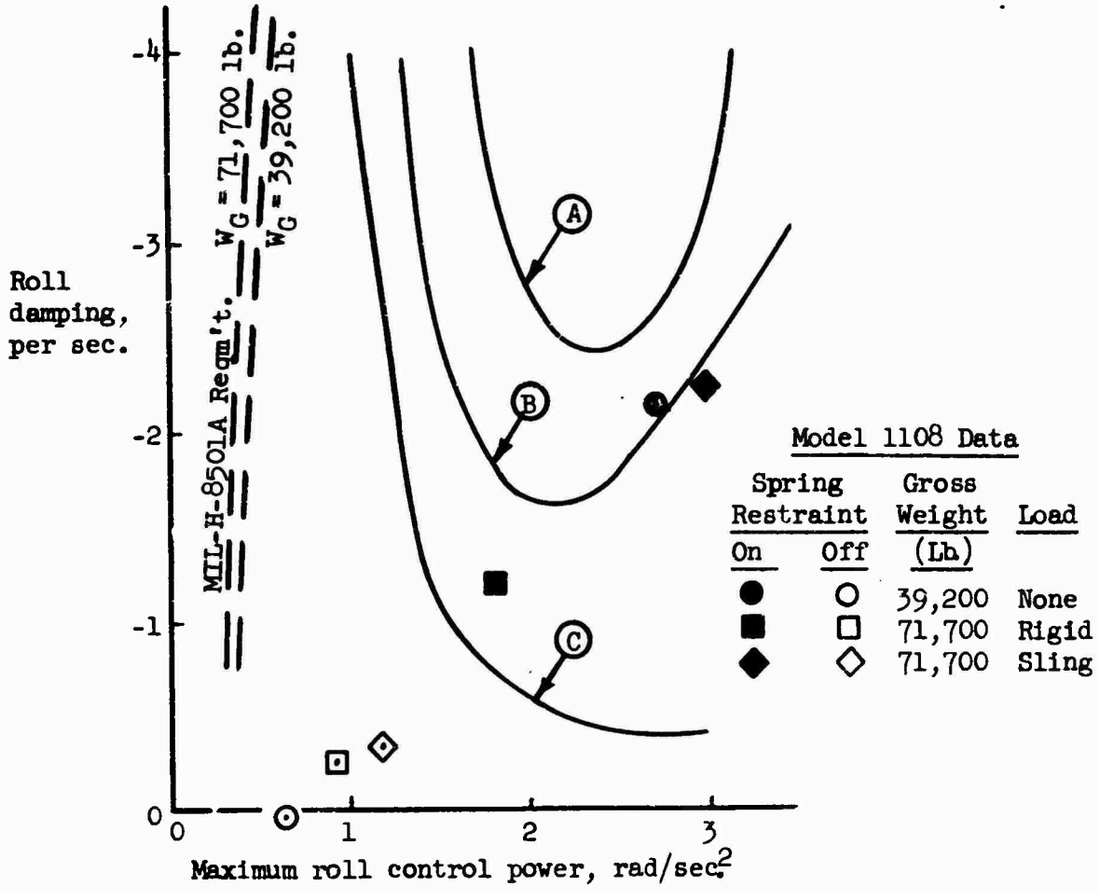

Figure 26. Maximum Control Power, Roll Axis.

Boundary	Descriptive Pilot Opinion	Reference
Ⓐ	"Desirable" - "good handling qualities for instrument flight operations"	NASA TN D-58, Ref. 8 (S-51 flight test)
Ⓑ	"Acceptable" - "acceptable for instrument flight operations"	
Ⓒ	"Marginal" - "acceptable for visual flight operations only"	

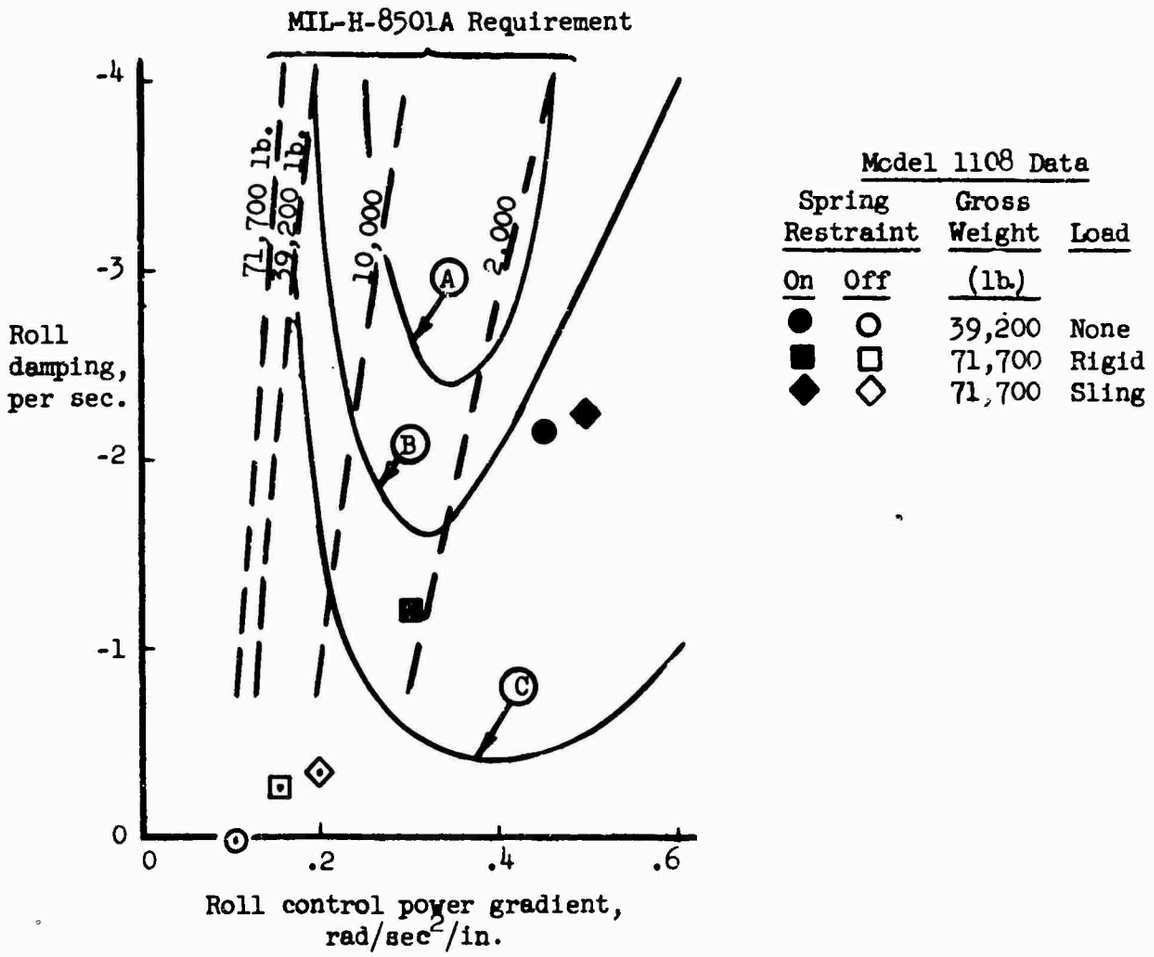

Figure 27. Control Power Gradient, Roll Axis.

Boundary	Descriptive Pilot Opinion	Reference
Ⓐ	"Desirable" - "good handling qualities for instrument flight operations"	NASA TN D-58 (Reference 8) (S-51 flight test)
Ⓑ	"Acceptable" - "acceptable for instrument flight operations"	
Ⓒ	"Marginal" - "acceptable for visual flight operations only"	

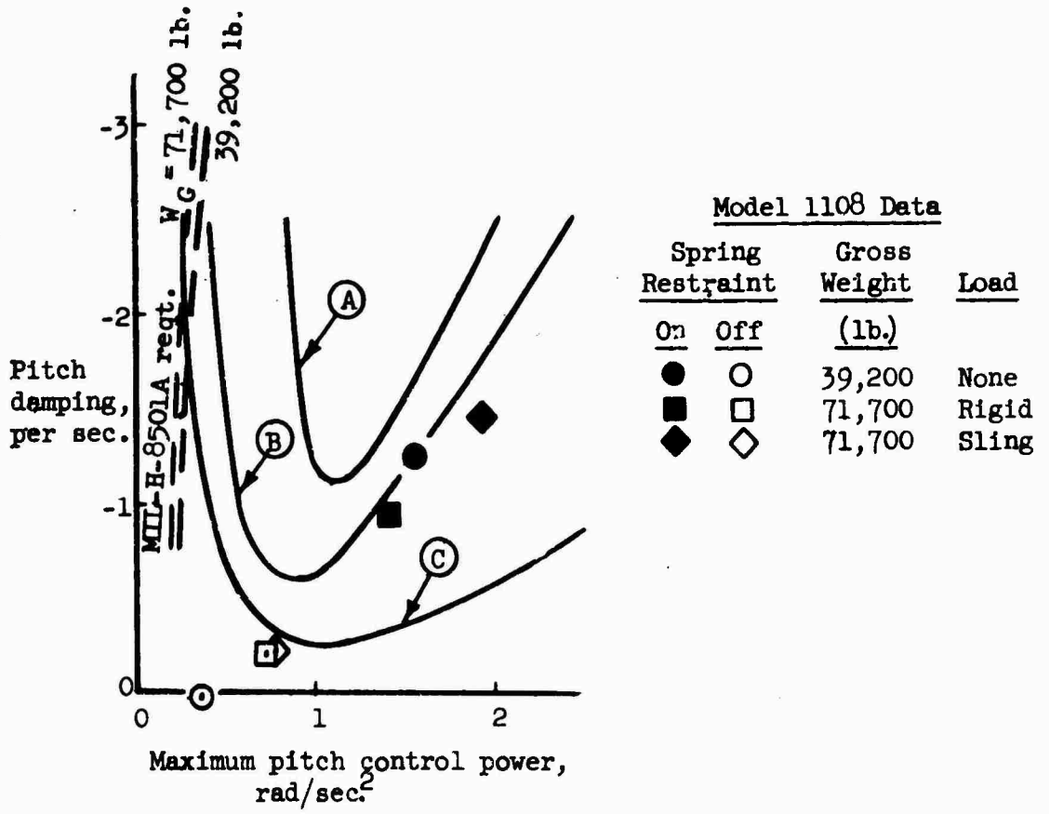

Figure 28. Maximum Control Power, Pitch Axis.

Boundary	Descriptive Pilot Opinion	Reference
Ⓐ	"Desirable" - "good handling qualities for instrument flight operations"	NASA TN D-58 (Reference 8) (S-51 flight test)
Ⓑ	"Acceptable" - "acceptable for instrument flight operations"	
Ⓒ	"Marginal" - "acceptable for visual flight operations only"	

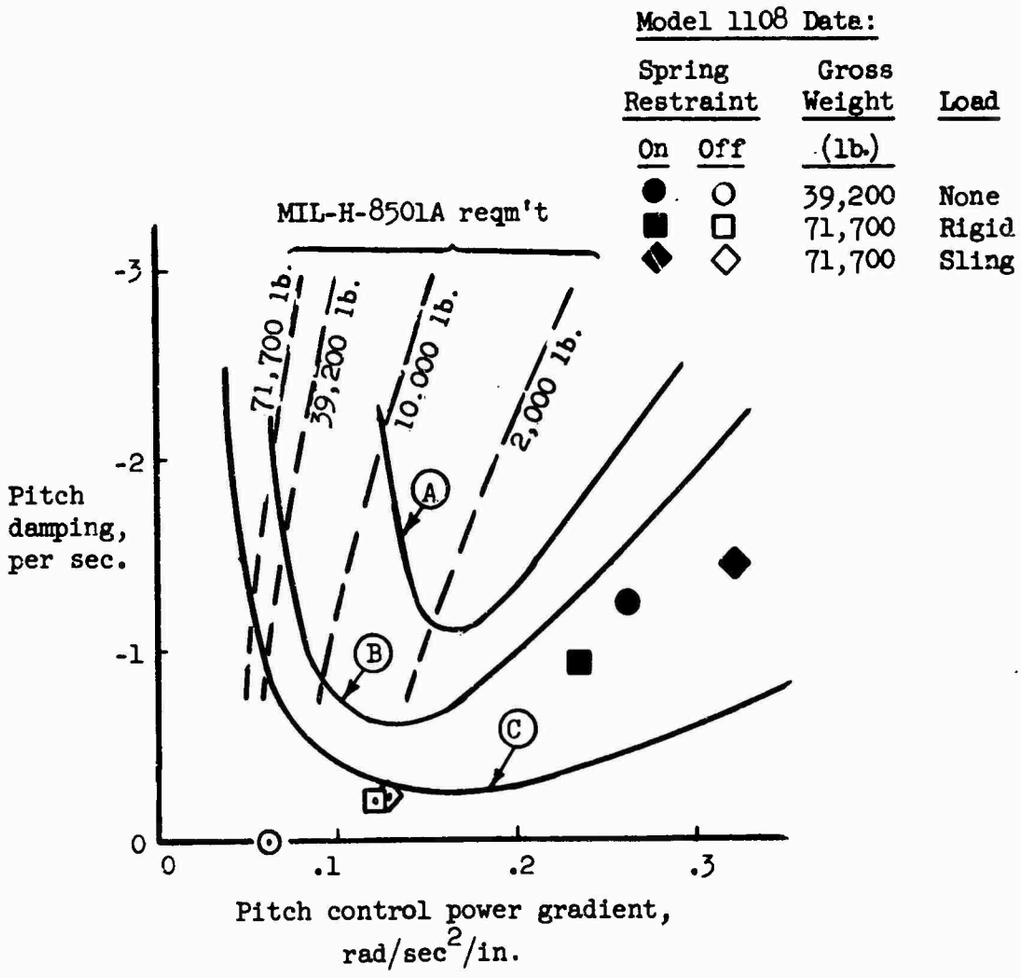

Figure 29. Control Power Gradient, Pitch Axis.

Unclassified

Security Classification

DOCUMENT CONTROL DATA - R&D

(Security classification of title, body of abstract and indexing annotation must be entered when the overall report is classified)

1. ORIGINATING ACTIVITY (Corporate author) Hiller Aircraft Company, Inc. Palo Alto, California	2a. REPORT SECURITY CLASSIFICATION Unclassified 2b GROUP

3. REPORT TITLE

Heavy-Lift Tip Turbojet Rotor System, "Stability and Control", Volume X

4. DESCRIPTIVE NOTES (Type of report and inclusive dates)

5. AUTHOR(S) (Last name, first name, initial)

6. REPORT DATE	7a. TOTAL NO. OF PAGES	7b. NO. OF REFS
October 1965	76	11

8a. CONTRACT OR GRANT NO.	9a. ORIGINATOR'S REPORT NUMBER(S)
DA-44-177-AMC-25(T) b. PROJECT NO. c. Task 1M121401D14412 d.	USAAVLABS Technical Report 64-68J 9b. OTHER REPORT NO(S) (Any other numbers that may be assigned this report) Hiller Engineering Report No. 64-50

10. AVAILABILITY/LIMITATION NOTICES

Qualified requesters may obtain copies of this report from DDC.
This report has been furnished to the Department of Commerce for sale to the public.

11. SUPPLEMENTARY NOTES	12. SPONSORING MILITARY ACTIVITY
	US Army Aviation Materiel Laboratories Fort Eustis, Virginia

13. ABSTRACT

Volume X of Heavy-Lift Tip Turbojet Rotor System discusses the results of a stability and control analysis of a large crane-type helicopter powered by a tip-mounted turbojet system. Specification MIL-H-8501A was used as a guide for criteria. Specification criteria were met; however, for improvements in handling qualities, a stability augmentation system is recommended.

DD FORM 1 JAN 64 1473

Unclassified

Security Classification

14. KEY WORDS	LINK A		LINK B		LINK C	
	ROLE	WT	ROLE	WT	ROLE	WT
Tip Turbojet Rotor System Stability and Control						

INSTRUCTIONS

1. ORIGINATING ACTIVITY: Enter the name and address of the contractor, subcontractor, grantee, Department of Defense activity or other organization *(corporate author)* issuing the report.

2a. REPORT SECURITY CLASSIFICATION: Enter the overall security classification of the report. Indicate whether "Restricted Data" is included. Marking is to be in accordance with appropriate security regulations.

2b. GROUP: Automatic downgrading is specified in DoD Directive 5200.10 and Armed Forces Industrial Manual. Enter the group number. Also, when applicable, show that optional markings have been used for Group 3 and Group 4 as authorized.

3. REPORT TITLE: Enter the complete report title in all capital letters. Titles in all cases should be unclassified. If a meaningful title cannot be selected without classification, show title classification in all capitals in parenthesis immediately following the title.

4. DESCRIPTIVE NOTES: If appropriate, enter the type of report, e.g., interim, progress, summary, annual, or final. Give the inclusive dates when a specific reporting period is covered.

5. AUTHOR(S): Enter the name(s) of author(s) as shown on or in the report. Enter last name, first name, middle initial. If military, show rank and branch of service. The name of the principal author is an absolute minimum requirement.

6. REPORT DATE: Enter the date of the report as day, month, year; or month, year. If more than one date appears on the report, use date of publication.

7a. TOTAL NUMBER OF PAGES: The total page count should follow normal pagination procedures, i.e., enter the number of pages containing information.

7b. NUMBER OF REFERENCES: Enter the total number of references cited in the report.

8a. CONTRACT OR GRANT NUMBER: If appropriate, enter the applicable number of the contract or grant under which the report was written.

8b, 8c, & 8d. PROJECT NUMBER: Enter the appropriate military department identification, such as project number, subproject number, system numbers, task number, etc.

9a. ORIGINATOR'S REPORT NUMBER(S): Enter the official report number by which the document will be identified and controlled by the originating activity. This number must be unique to this report.

9b. OTHER REPORT NUMBER(S): If the report has been assigned any other report numbers *(either by the originator or by the sponsor)*, also enter this number(s).

10. AVAILABILITY/LIMITATION NOTICES: Enter any limitations on further dissemination of the report, other than those imposed by security classification, using standard statements such as:

(1) "Qualified requesters may obtain copies of this report from DDC."

(2) "Foreign announcement and dissemination of this report by DDC is not authorized."

(3) "U. S. Government agencies may obtain copies of this report directly from DDC. Other qualified DDC users shall request through _____."

(4) "U. S. military agencies may obtain copies of this report directly from DDC. Other qualified users shall request through _____."

(5) "All distribution of this report is controlled. Qualified DDC users shall request through _____."

If the report has been furnished to the Office of Technical Services, Department of Commerce, for sale to the public, indicate this fact and enter the price, if known.

11. SUPPLEMENTARY NOTES: Use for additional explanatory notes.

12. SPONSORING MILITARY ACTIVITY: Enter the name of the departmental project office or laboratory sponsoring *(paying for)* the research and development. Include address.

13. ABSTRACT: Enter an abstract giving a brief and factual summary of the document indicative of the report, even though it may also appear elsewhere in the body of the technical report. If additional space is required, a continuation sheet shall be attached.

It is highly desirable that the abstract of classified reports be unclassified. Each paragraph of the abstract shall end with an indication of the military security classification of the information in the paragraph, represented as *(TS)*, *(S)*, *(C)*, or *(U)*.

There is no limitation on the length of the abstract. However, the suggested length is from 150 to 225 words.

14. KEY WORDS: Key words are technically meaningful terms or short phrases that characterize a report and may be used as index entries for cataloging the report. Key words must be selected so that no security classification is required. Identifiers, such as equipment model designation, trade name, military project code name, geographic location, may be used as key words but will be followed by an indication of technical context. The assignment of links, rules, and weights is optional.